LONG TERM DEFLECTIONS OF REINFORCED CONCRETE FLEXURAL ELEMENTS

GUY STANLEY CLARKE

A project report submitted to the Faculty of Engineering, University of the Witwatersrand, Johannesburg, in partial fulfilment of the requirements for the degree of Master of Science in Engineering

Johannesburg, 1986

LIST OF TABLES

DECLARATION

I, Guy Stanley Clarke, hereby declare that this project is my own unaided work, and has not been submitted before for any degree or examination in any other University.

. . . .

26th day of November 1986.

Page

ABSTRACT

Many methods have been proposed for the calculation of long term deflections in reinforced concrete members. Most methods make use of empirical factors to modify instantaneous deflection in calculating long term deflection. In this study a semi-theoretical method of long term deflection calculation is derived from a consideration of midspan strain changes and the stress redistribution accompanying creep. The predictions of this calculation method are compared with deflections and strains measured on four reinforced concrete beams subjected to sustained loading for a duration of six months. The method is shown to give good results in predicting long term deflection from measured concrete properties.

LIST OF SYMBOLS

A_s - Area of tension reinforcement

A_s' - Area of compression reinforcement

α_e - Modular ratio = E_s/E_c

b - Width of section

d - Effective depth of tension reinforcement

Δ_c - Creep deflection

Δ_i - Instantaneous or immediate deflection

Δ_{sh} - Shrinkage deflection

Δ_t - Deflection at time t (in days)

E_c - Static secant modulus of elasticity of concrete

E_s - Modulus of elasticity of steel

ϵ_c - Compression strain

ϵ_{cr} - Creep strain

ϵ_s - Tensile strain

ϵ_{sh} - Shrinkage strain

f_c - Concrete compressive stress in extreme compression fibre

f_{cu} - Characteristic concrete cube strength

f_{cyl} - Measured concrete cylinder strength

f_c' - Characteristic concrete cylinder strength

$f_{meas.}$ - Measured concrete cube strength

f_r - Modulus of rupture (concrete)

ϕ_{ct} - Creep coefficient (measured on prisms)

ϕ'_{ct} - Creep coefficient in beam extreme compression fibre

h - Overall depth of section in plane of bending

I_{cr} - Second moment of area of cracked section

I_e - Effective second moment of area

I_g - Second moment of area of concrete section only

I_{tr} - Second moment of area of transformed section

k - Constant defined by load arrangement (used in deflection calculation)

l - Beam length

CONTENTS

M_{cr} - Minimum moment causing cracking in beam tension zone

M_a - Applied moment

ρ - $\rho = A_s/bd$

ρ' - $\rho' = A_s'/bd$

ρ_o - Constant depending on ρ and ρ' used in shrinkage deflection calculation (from CP110)

$1/r$ - Beam curvature

s_ϕ - Stress ratio in extreme compression fibre at creep = ϕ. $(s_\phi = (f_c)_t/(f_c)_i)$

t - Time in days

x - Ratio of neutral axis depth to effective depth of section

y_t - Distance from neutral axis to extreme tension fibre

NOTE: t may be used as a subscript to any of the above symbols or replaced by a numeral representing a specific time in days. Subscript i is similarly used to denote "immediate" or "instantaneous".

Additional symbols used are defined in the text where appropriate.

1. INTRODUCTION

The long term deflection of reinforced concrete flexural elements has been widely researched and many methods have been proposed for deflection calculation. Despite this, a wide range of *results can be derived* using different calculation methods. Most methods are empirically based and have been derived from limited experimental observation. As a result their universal applicability is questionable. (A detailed examination of some of these calculation methods is undertaken in Chapter 2).

In many reinforced concrete structures no deflection check is required at all. For the vast majority it is adequate to follow the span/effective depth rules prescribed by codes to limit deflections. However, situations do arise where deflections are critical and more accurate calculations are justified. In such instances the designer has very little guidance in the selection of calculation method. A more widely applicable method is required. It is believed that wider applicability can best be achieved by closer *theoretical correlation*.

Immediate or short term deflections can be accurately predicted by most current codes of practice such as CP110[1] or ACI 318[2], making use of the partially cracked section concept. The problem presented by long term deflection calculation is twofold. The relevant concrete properties (modulus of elasticity, creep and shrinkage) have to be measured or calculated from the known basic parameters (mix constituents, compressive strength and environmental conditions). These

Page

APPENDICES

properties and the characteristics of the reinforced concrete element under consideration are then used to calculate deflection. Creep and shrinkage data for a particular concrete is seldom available, and if it is, it is most unlikely that it will cover the lifetime of a structure. Extrapolation from shorter term data is invariably necessary. Because of the variability of concrete creep and shrinkage characteristics, some prior measurement of these values is essential for accurate deflection calculation. In this investigation emphasis is concentrated on deflection calculation from measured creep and shrinkage parameters, ther than the prediction of these concrete properties.

The question of whether the effects of shrinkage and creep should be separated or combined is often debated. Most calculation methods make use of a coefficient representing the ratio of long term to initial deflection. If initial deflection tends to zero the creep portion of long term deflection will also necessarily tend to zero, while the shrinkage portion remains largely unaffected, so an overall coefficient will tend to infinity. In the extreme case where the initial deflection and creep deflection are zero, shrinkage deflection cannot be calculated by such a coefficient. Creep is dependent on the level of applied loading, but shrinkage is not. Although it is acknowledged that shrinkage and creep may be part of the same phenomenon, it is essential to separate their effects for accurate deflection calculation if the coefficient approach is used.

The results of previous researchers are not readily useable in a comprehensive deflection study. Little attention has been given to strains across element

LIST OF FIGURES

sections. Where strain measurements have been made these are generally not analysed in detail and are very seldom reported in sufficient detail so as to be useable by others. Shrinkage and creep effects are not always separated and not always measured on companion prisms of the same concrete. Span/effective depth ratios are often unrealistic when compared with current code recommendations. If shrinkage effects are to be separated it is essential to measure shrinkage deflection on a similar cracked reinforced concrete member. Reported results very often contain insufficient detail for a subsequent in depth study, although more detail could no doubt be obtained by direct contact with the educational institution or individual concerned. The problems outlined above are evidant in the study of other research results undertaken in Chapter 6.

The objectives of this investigation may be summarized as follows:

(1) To examine both theoretically and experimentally the development of strains with time across the sections of rectangular reinforced concrete beams subjected to sustained loading.

(2) To relate strain development to short and long term concrete properties measured on control prisms.

(3) To derive a method of long term deflection calculation using concrete properties measured on control prisms. The method derived should be compatible with both theory and observed results.

Page

Shrinkage and creep effects are separated where possible. More attention is given to creep than shrinkage as creep is generally the major contributing factor to long term deflections.

A theoretically derived method of long term deflection calculation is presented in this report. The *theoretical hypotheses upon which the method is based* are compared with experimental results. Deflections calculated by this method and other popular methods are compared with deflections measured in this and other research programmes.

Tables of measured data are included in the appendices. The results have been computer processed and are presented in computer print-out format. Data relevant to the argument of the main te[illegible]peated there for ease of reference. Me[illegible] data has been comprehensively tabled to [illegible]ite use by other investigators.

Where possible the symbols of CP110 or SABS 0100[3] are used. In the absence of particular symbols being specified in those documents, the symbols most commonly used in related literature have been adopted.

2. LITERATURE STUDY - AN EVALUATION OF EXISTING METHODS OF LONG TERM DEFLECTION CALCULATION

An evaluation of existing methods of long term deflection calculation is necessary to provide substantiation for criticism levelled at these methods and to introduce some established concepts relevant to any long term deflection study.

It was noted in the introduction (Chapter 1) that attention is focused primarily on long term deflection, and creep deflection in particular, in this study. The calculation of instantaneous or immediate deflection, shrinkage deflection and concrete properties relevant to long term deflection calculation is not covered in this chapter except in so far as it directly affects long term deflection due to creep.

It is impossible to give each calculation method comprehensive coverage in the limited space available. The methods described are generally well known and more detailed descriptions of their prescribed application are readily accessible in the references quoted. In general the symbols used in the equations repeated here are identical to those in these references and are defined in the text. Some of these symbols are peculiar to this chapter and may be defined differently under "List of Symbols" on page (x). In such cases the definition given here is only applicable in this chapter.

Three basic methods of calculation are covered. These methods can in principle be considered representative of the many methods presented in deflection literature.

2.1 CP110, 1972[1]

The method prescribed by CP110 makes use of modular ratio techniques (elastic analysis) for the calculation of x_i (here only, x = neutral axis depth) and I_i. x_t and I_t are calculated by considering a reduced elastic modulus

$$E_{ct} = E_{ci}/(1 + \phi_{ct}) \qquad (2.1)$$

and increased modular ratio

$$\alpha_{et} = E_s/E_{ct} = (1 + \phi_{ct})\alpha_{ei} \qquad (2.2)$$

Parameters x_i, I_i, x_t and I_t are all calculated assuming the concrete section to be completely cracked. For both instantaneous and long term deflections the effect of concrete in tension (tension stiffening) is introduced directly in the curvature calculation. For a rectangular section:

$$\text{curvature} = 1/r = \frac{M - A}{EI} \qquad (2.3)$$

$$\text{where } A = \frac{(h - x)\ .\ bf_{ct}}{(d - x)\ .\ 3} \qquad (2.4)$$

and caters for tension stiffening.

$$\text{Then } \Delta = k.(1/r)\ l^2 \qquad (2.5)$$

where k is a constant dependant on the arrangement of applied loads.

Values of k can be derived from the classical elastic theory equation

$$\frac{d^2y}{dx^2} = \frac{M}{EI} \qquad (2.6)$$

and are tabulated in several references for most common load cases[4][5].

f_{ct} represents the concrete strength in tension at the level of tension reinforcement and varies between 1,0 MPa (instantaneous deflection) and 0,55 MPa (extreme long term deflection). Intermediate values are tabulated in reference[4]. This table is repeated here (Table 2.1) for information. It will be noted that creep coefficient and tensile stress in concrete are tabulated against duration of load. If the creep coefficient is measured it is probably better to determine f_{ct} from the coefficient than from the duration of load.

Table 2.1 Creep coefficients and reduction with time of stress in concrete at steel level[4]

Duration of load (days)	Age at loading (days)					f_{ct} (MPa)
	7	14	28	56	100	
0	0	0	0	0	0	1,00
10	0,36	0,33	0,27	0,23	0,19	0,95
100	1,92	1,65	1,37	1,17	0,96	0,77
1000	3,08	2,64	2,20	1,87	1,54	0,64
∞	3,85	3,30	2,75	2,34	1,93	0,55

Equations 2.3 and 2.4 are derived from the stress diagram illustrated in Figure 2.1. Shrinkage deflection is calculated separately.

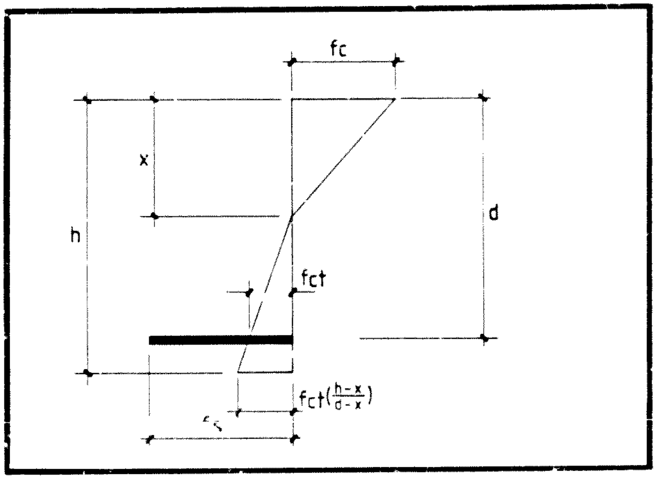

Figure 2.1 Stresses through depth of concrete section - allowance for tension stiffening

The legitimacy of the application of modular ratio techniques to the calculation of long term section properties and deflection may be doubtful. It is often claimed that the CP110 calculation tends to underestimate long term deflections because the increase in α_e and decrease in E_c with creep have a cancelling effect. Comparison of measured deflections with CP110 calculated deflections tends to confirm this[6][7].

Th[illegible] term catering for *tension stiffening* (equation 2.4) is [illegible]rical and is not related to the level of applied moment. This may limit the range of applicability of this method because concrete tension zone cracking increases (i.e. tension stiffening decreases) with an increase in applied moment.

2.2 ACI 318 - 1983[2]

The provisions of the ACI code are based upon the experimentally derived moment-curvature relationship illustrated in Figure 2.2. From this figure it is evident that an abrupt change occurs at the point at which first cracking occurs in the concrete tension zone. Up to this point (1/r) is proportional to $1/I_{tr}$ where I_{tr} is the moment of inertia of the uncracked transformed section. Thereafter (1/r) is proportional to $(1/I_e)$ where I_e is an effective moment of inertia allowing for cracking in the concrete tension zone. In Figure 2.2 $(1/I_e)$ is proportional to the slope of the line joining the origin and point 'a'. I_e varies with the magnitude of the applied moment and is calculated by equation 2.7.

$$I_e = \left(\frac{M_{cr}}{M_a}\right)^3 I_g + \left(1 - \left(\frac{M_{cr}}{M_a}\right)^3\right) I_{cr} \qquad (2.7)$$

where M_a = applied moment
M_{cr} = moment at first cracking
I_g = second moment of area of gross concrete section
I_{cr} = second moment of area of fully cracked section

The term catering for tension stiffening (equation 2.4) is empirical and is not related to the level of applied moment. This may limit the range of applicability of this method because concrete tension zone cracking increases (i.e. tension stiffening decreases) with an increase in applied moment.

2.2 ACI 318 - 1983[2]

The provisions of the ACI code are based upon the experimentally derived moment-curvature relationship illustrated in Figure 2.2. From this figure it is evident that an abrupt change occurs at the point at which first cracking occurs in the concrete tension zone. Up to this point (1/r) is proportional to $1/I_{tr}$ where I_{tr} is the moment of inertia of the uncracked transformed section. Thereafter (1/r) is proportional to $(1/I_e)$ where I_e is an effective moment of inertia allowing for cracking in the concrete tension zone. In Figure 2.2 $(1/I_e)$ is proportional to the slope of the line joining the origin and point 'a'. I_e varies with the magnitude of the applied moment and is calculated by equation 2.7.

$$I_e = \left(\frac{M_{cr}}{M_a}\right)^3 I_g + \left(1 - \left(\frac{M_{cr}}{M_a}\right)^3\right) I_{cr} \qquad (2.7)$$

where M_a = applied moment

M_{cr} = moment at first cracking

I_g = second moment of area of gross concrete section

I_{cr} = second moment of area of fully cracked section

$$\text{Then } (1/r)_i = \frac{M}{EI_e} \qquad (2.8)$$

$$\text{and } \Delta_i = k.(1/r)_i l^2 \qquad (2.9)$$

$$M_{cr} = \frac{f_r \, I_g}{y_t} \qquad (2.10)$$

where f_r = modulus of rupture (tensile strength) of concrete

$$f_r = 0,7\sqrt{f_c'} \qquad (2.11)$$

where f_c' = characteristic concrete cylinder strength

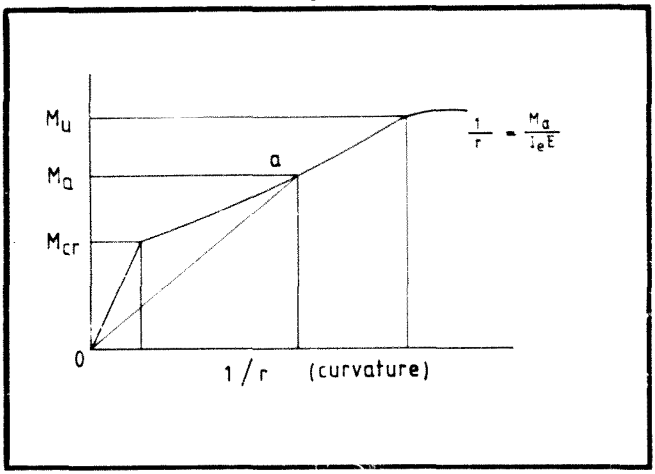

Figure 2.2 Moment curvature relationship for reinforced concrete beam

In equations 2.7 and 2.10 I_{tr} has been replaced by the slightly smaller I_g, probably to simplify calculations.

Additional *long term deflection* is calculated by multiplying Δ_i by λ.

$$\lambda = \frac{\Omega}{1 + 50\rho'} \tag{2.12}$$

The quotient in 2.12 is Branson's coefficient[8] catering for compression reinforcement. Factor Ω is specified in the code.

$$\Delta_t = (1 + \lambda)\,\Delta_i \tag{2.13}$$

Δ_t thus calculated includes shrinkage. No allowance is made for the separate calculation of *shrinkage* and creep, nor is any provision made for the introduction of a measured creep coefficient.

The use of *an effective* moment of inertia gives very good results in the calculation of short term deflections. The application of a single multiplier (λ) to short term deflection to derive *long term* deflection presents a gross oversimplification of the situation. In defence of the code, however, it should be noted that accuracy has been sacrificed for simplicity, and its *provisions* are certainly easy to interpret and apply. It was clearly never the intention of the authors to provide a sophisticated calculation method for critical deflection situations.

An approach described by Neville[5] is very similar, but relies more on measured parameters.

From Neville:

$$f_r = 0,6\sqrt{f_{cyl}} \qquad (2.14)$$

where f_{cyl} = average cylinder strength (measured)

and $$\Delta_t = \Delta_i (1 + K_\phi \phi_t) \qquad (2.15)$$

where K_ϕ is an empirical factor.

Neville suggests that for creep (*i.e. shrinkage excluded*) the following expressions may be adopted for K_ϕ

$$\rho \leq 0.007 \quad : \quad K_\phi = \frac{0,85}{1 + 50\rho'} \qquad (2.16)$$

(*adopted from* Branson[8])

$\rho > 0,007$:

$$K_\phi = \frac{\sqrt{(100\rho\alpha_e)}}{12\ (1 + \rho'/\rho)} \qquad (2.17)$$

(adopted from Mayer[9])

It is also recommended by *Neville* that *shrinkage* be calculated separately, although Branson[8] has suggested that total long term deflection (including shrinkage) can be calculated using equation 2.16 by changing the 0,85 factor to 1,0

The range of applicability of Neville's recommendation is improved by *the use of different* factors for different ρ values, but is still severely limited.

Consider K_ϕ for ρ = 0,007 = ρ'

Take α_e = 210/30 = 7 (*typical value*)

From 2.16 K_ϕ = 0,630

From 2.17 K_ϕ = 0,092

The discrepancy speaks for itself.

Other methods of calculating I_e do exist[10] but give essentially the same result in evaluating short term deflections.

2.3 SAICE RECOMMENDATION - PRETORIUS[6]

The Deflection Sub-Committee of the Structural Division of the South African Institution of Civil Engineers recently published a report in which a different approach to long term deflection calculation is advocated. The method is based upon modular ratio techniques and the development of strains due to creep in the fully cracked concrete section.

Figure 2.3 illustrates the idealized strain distribution through a fully cracked, singly reinforced beam. C_t represents the concrete creep coefficient at time t.

Equating similar triangles:

$$x_t = \frac{x_i(1 + C_t)}{(1 + x_i C_t)} \qquad (2.18)$$

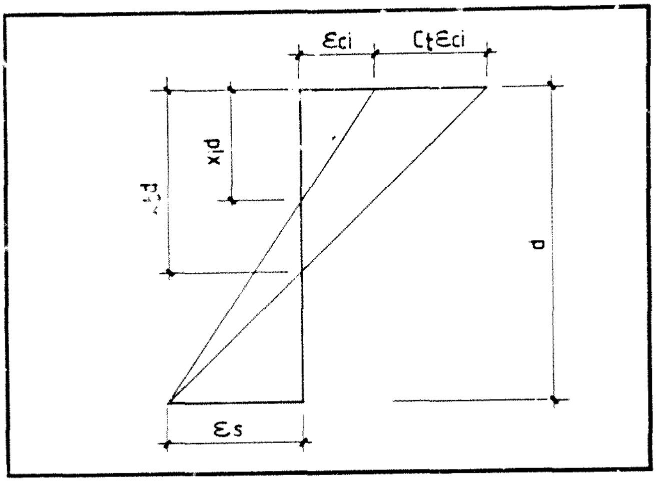

Figure 2.3 Idealized strain distribution through beam section (instantaneous and long term - fully cracked section)

From the cracked transformed section (using modular ratio technique):

$$\alpha_{et} = \frac{x_t^2}{2\rho(1 - x_t)} \qquad (2.19)$$

I_{cr} can be calculated using α_{et} from 2.19:

$$\frac{(I_{cr})_t}{bd^3} = \frac{x_t^2}{2} - \frac{x_t^3}{6} \qquad (2.20)$$

$$\text{and} \quad \frac{(EI_{cr})_i}{(EI_{cr})_t} = \frac{\Delta_t}{\Delta_i} = \frac{(1 + x_i C_t)^2}{1 + 2x_i C_t/(3 - x_i)} \qquad (2.21)$$

For sections with compression steel more complex equations are derived. However, for simplicity it is recommended by Pretorius that equation 2.21 be used with an adjusted C_t given by

$$C_t' = C_t.(1 - \rho'/(2\rho)) \qquad (2.22)$$

No recommendation is made for the separation of shrinkage and creep effects.

This calculation method has been shown (6) to give very good results in predicting total long term deflections using a measured prism creep coefficient or a creep coefficient determined by the method of reference (11). However, several important facts are overlooked in its derivation.

1) The method is derived from the completely cracked beam section. It is generally accepted that some allowance should be made for tension stiffening. (This issue is discussed in more detail in Chapter 3)

2) It has been shown (7)(12)(13) that creep in the extreme compression fibre is somewhat less than that measured on axially loaded prisms. This suggests that C_t should be factored (by a value less than unity).

3) Creep coefficient is used to predict total deflection (i.e. creep and shrinkage). As noted in Chapter 1, the effects of creep and shrinkage should ideally be separated if the coefficient approach is used. Creep coefficient should be used to predict creep deflections only.

3. DERIVATION OF PROPOSED CALCULATION METHOD

Possibly the most significant criticism that can be made of existing methods of long term deflection calculation is that their derivation is too reliant on experimental observation. Few attempts have been made to correlate the observed results with theoretical calculations. As a result these methods are *unlikely to* be universally applicable. The derivation of a calculation method compatible with both theory and observed results appears to present a logical approach if wider applicability is to be achieved.

The following general observations have been made in the research results studied:[(7),(12),(13)].

(1) Plane sections across the depth of the reinforced concrete element remain essentially plane after the application of loads.

(2) Creep results in an increase in neutral axis depth.

(3) The creep coefficient in the extreme compression fibre (measured as creep strain divided by initial strain) is somewhat less than that measured on uniformly loaded control prisms in the same storage environment. Bayazid and Pauw[(14)] concluded from tests on eccentrically loaded prisms that the application of a triangularly distributed stress (as opposed to a uniformly distributed stress) makes no difference to the resulting creep coefficient. The reduced creep coefficient in the extreme compression fibre must therefore result from the stress decrease in the extreme fibre caused by the increased neutral axis depth accompanying creep.

(4) Measured strain at the level of the tension reinforcement is initally much less than the value calculated assuming a completely cracked section (using modular ratio techniques), but very rapidly approaches or exceeds that value under the application of sustained loading. This effect must result from the rapid development of cracking in the concrete tension zone.

It is unlikely that crack development is due to creep alone. It is probably due to a combination of mechanisms which include:

(i) Increased tensile stress in the concrete resulting from the lowering of the neutral axis accompanying creep. (The greater neutral axis depth results in a reduction in the lever arm of the internal forces resisting the applied moment. With a reduced lever arm larger forces are required to resist the same moment).

(ii) A reduction in the effective concrete tensile strength with time [(1),(19)].

(iii) Shrinkage cracking caused by the reinforced concrete element being restrained or partially restrained at its supports and by the tension reinforcement.

Since the attainment of the completely cracked condition is only partially dependent on concrete creep, it may be sufficient to consider creep effects applied to the completely cracked section in considering strain development under long term loading. This approach has been adopted by Pretorius[6].

Strains through the depth of the *completely* cracked section are shown schematically in Figure 3.1. Load application results in initial strains ϵ_{ci} and ϵ_{si} (or ϵ_s) in the extreme compression fibre and at the level of the *tension reinforcement* respectively. With creep the strain in the extreme compression fibre becomes $\epsilon_{ct} = (1 + \phi'_{ct})\epsilon_{ci}$. ϕ'_{ct} is the creep coefficient in the extreme compression fibre at time t. The *neutral axis* depth increases from $x_i d$ to $x_t d$ with creep. x represents the ratio of neutral axis depth to the effective depth of the section.

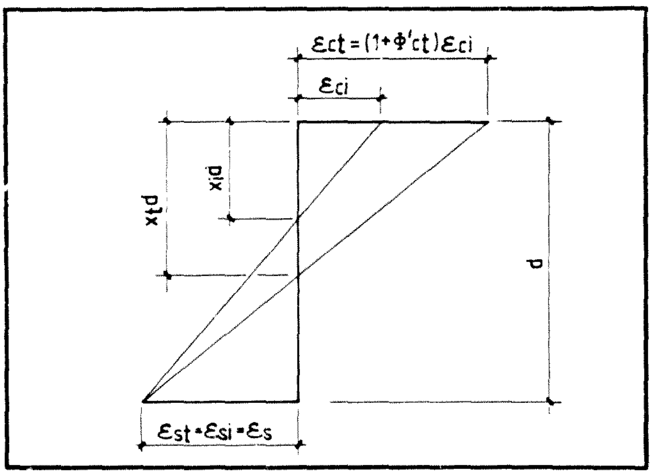

Figure 3.1 Idealized strain distribution through fully cracked beam section

It has been assumed that the tensile strain at the level of the tension reinforcement is *equal* to the cracked section value and is unaffected by creep. In practice the tensile strain increases marginally due to the increase in neutral axis depth accompanying creep. At the same time however, it is probable that some degree of tension stiffening (however small) by the concrete in the tension zone remains. The increased tensile strain may be wholly or partially offset by the residual tension stiffening effect. The assumption of a constant tensile strain equal to the cracked section value thus appears reasonable, even though it is quantitatively unsubstantiated.

Considering Figure 3.1.

$$\text{Curvature} = (1/r) \propto \Delta \text{ (deflection)}$$

$$(1/r)_i = \frac{\epsilon_{ci} + \epsilon_s}{d} \qquad (3.1)$$

$$(1/r)_t = \frac{\epsilon_{ct} + \epsilon_s}{d} \qquad (3.2)$$

$$= \frac{\epsilon_{ci}(1 + \phi'_{ct}) + \epsilon_s}{d} \qquad (3.3)$$

Therefore:

$$(1/r)_t/(1/r)_i = \frac{\epsilon_{ci}(1 + \phi'_{ct}) + \epsilon_s}{\epsilon_{ci} + \epsilon_s} \qquad (3.4)$$

ϕ'_{ct} represents the creep coefficient in the extreme compression fibre, as distinct from ϕ_{ct}, the creep coefficient measured on axially loaded specimens.

Now:

$$\frac{\epsilon_s}{d - x_i d} = \frac{\epsilon_{ci}}{x_i d} \qquad (3.5)$$

$$\epsilon_s = \epsilon_{ci}(1 - x_i)/x_i \qquad (3.6)$$

Substituting for ϵ_s in (3.4) gives:

$$\Delta_t/\Delta_i = (1/r)_t/(1/r)_i = 1 + x_i\phi'_{ct} \qquad (3.7)$$

The above provides a simple method of calculating long term deflection (Δ_t) from the initial cracked section deflection (Δ_i) provided ϕ'_{ct} is known.

It is known that ϕ'_{ct} becomes progressively smaller than the measured prism creep *coefficient* (ϕ_{ct}) as the neutral axis depth *increases* i.e. as creep progresses.

From Pretorius[(6)] (derived by considering similar *triangles* in Figure 3.1.):

$$x_t = \frac{x_i\ (1 + \phi'_{ct})}{1 + x_i\ \phi'_{ct}} \qquad (3.8)$$

M (moment) $= 0{,}5 . f_c\ b\ d^2\ x\ (1 - {}^x/_3)$

where $d(1 - {}^x/_3)$ is the lever arm and f_c is the extreme compression fibre stress. Since M is constant ($M_i = M_t$)

$$\frac{(f_c)_t}{(f_c)_i} = \frac{x_i(1 - {}^{x_i}/_3)}{x_t(1 - {}^{x_t}/_3)} \qquad (3.9)$$

Substituting for x_t in (3.9) gives

$$\frac{(f_c)_t}{(f_c)_i} = \frac{(3 - x_i)(1 + x_i\,\phi'_{ct})^2}{(1 + \phi'_{ct})(3 - x_i + 2x_i\phi'_{ct})} \qquad (3.10)$$

The relationship of (3.10) is not as simple as it appears at first sight. ϕ'_{ct} is not a constant but increases as creep takes place (i.e. as ϕ_{ct} increases). However, $(f_c)_t$ decreases with time, so that creep in the beam occurs under conditions of reducing stress, with the result that ϕ'_{ct} decreases below the value of ϕ_{ct}. A numerical solution to (3.10) is applied here.

If we take x_i = 0,4 (typical value) then (3.10) reduces to:

$$\frac{(f_c)_t}{(f_c)_i} = \frac{2,6(1 + 0,4\phi'_{ct})^2}{(1 + \phi'_{ct})(2,6 + 0,8\phi'_{ct})} \qquad (3.11)$$

The solution is derived by considering increasing values of ϕ_{ct} from ϕ_{ct} = 0 in a stepwise fashion, and will depend on the $\Delta\phi_{ct}$ values used - smaller values will give greater accuracy. It is easier to express $(f_c)_t/(f_c)_i$ as a function of ϕ than as a function of time for calculation purposes. For convenience this ratio is expressed as s_ϕ (stress ratio at creep = ϕ).

It is necessary to consider a number of creep intervals of magnitude $\Delta\phi_{ct}$. During the first interval ϕ'_{ct} must have the same value as ϕ_{ct} as $(f_c)_t / (f_c)_i = 1$ (i.e. creep must occur to induce a stress reduction in the beam extreme compression fibre)

For example:

using $\Delta\phi_{ct} = 1,0$

and therefore $\phi'_{c1} = 1,0 = \phi_{c1}$

From (3.11) $s_1 = (f_c)_1/(f_c)_i = 0,749$

For the second period of creep (as ϕ_{ct} increases from 1,0 to 2,0), the creep coefficient in the beam extreme compression fibre will increase from 1,0 to 1,749 as the stress in the extreme fibre is reduced to 74,9% of the initial stress.

$$\text{i.e.}\quad \phi_{c2} = \phi_{c1} + \Delta\phi_{ct} = 1,0 + 1,0 = 2,0$$

$$\phi'_{c2} = s_0\,\Delta\phi_{ct} + s_1\,\Delta\phi_{ct}$$

$$= \Delta\phi_{ct}\,(s_0 + s_1)$$

$$= 1,0\ (1,0 + 0,749)$$

$$= 1,749$$

Using $\phi'_{c2} = 1,749$ in 3.11 we get

$$s_2 = (f_c)_2/(f_c)_1 = 0,683$$

Then $\phi'_{c3} = \Delta\phi_{ct}\,(s_0 + s_1 + s_2)$

$$= 1,0\ (1,0 + 0,749 + 0,683)$$

$= \quad 2,432$

and $\phi_{c3} \quad = \quad 3,0 . \Delta\phi_{ct} \quad = \quad 3,0$

Values of ϕ'_{ct} versus $_{ct}$ calculated using different $\Delta\phi_{ct}$ values are listed in Table 3.1. It is evident from the table that ϕ'_{ct} is relatively insensitive to the $\Delta\phi_{ct}$ value used provided several calculation cycles have been performed.

Table 3.1 ϕ'_{ct} calculated for different $\Delta\phi_{ct}$ values (x_i = 0,4)

$\Delta\phi_{ct}$	Measured prism creep coefficient, ϕ_{ct}					
	1	2	3	4	5	6
1,0	1,000	1,749	2,432	3,081	3,708	4,320
0,5	0,916	1,655	2,334	2,980	3,606	4,217
0,1	0,866	1,595	2,270	2,914	3,538	4,148
0,01	0,856	1,583	2,257	2,901	3,524	4,134

From the above description of the calculation method it is evident that the ϕ'_{ct} value derived is an upper-bound value. For each creep period considered, beam extreme fibre creep is calculated from the stress ratio (s_ϕ) applicable at the start of that period. Since s_ϕ decreases with time, extreme fibre creep is overestimated.

In order to evaluate the accuracy of the calculation method it is also necessary to derive a lower-bound solution. If we calculate beam extreme fibre creep from the stress ratio (s_ϕ) applicable at the end of each creep period:

Then: $\phi'_{c3} = \Delta\phi_{ct} (s_1 + s_2 + s_3)$

and $\phi'_{cn} = \Delta\phi_{ct} (s_1 + s_2 + \ldots\ldots\ldots + s_n)$ (3.12)

For the upper-bound solution:

$$\phi'_{cn} = \Delta\phi_{ct} (s_0 + s_1 + \ldots\ldots\ldots + s_{n-1}) \quad (3.13)$$

If the difference between the two calculated values is denoted by δ:

$$\delta = \Delta\phi_{ct} (s_0 - s_n). \quad (3.14)$$

Strictly speaking, ϕ'_{ct} differs in the upper and lower-bound solutions, so s_i must differ in equations 3.12 and 3.13. s_ϕ decreases as ϕ increases, so s_i values in 3.13 (upper-bound) should be smaller than the corresponding values in 3.12 (lower-bound). Assuming that these values are equal produces the conservative solution of 3.14

Considering some examples:

(1) $\Delta\phi = 1,0$: ϕ prism $= 3,0$

$\phi'_c = 2,432$ (upper-bound)

$\delta = 1,0\ (1,0 - 0,649)$

$= 0,351$

ϕ'_c *(lower-bound)* $= 2,432 - 0,351$

$= 2,081$

i.e. The actual value of ϕ'_c lies between 2,081 and 2,432.

(2) $\Delta\phi = 0{,}1$: ϕ prism $= 4{,}0$

(The value quoted below for s_n is taken from a computer print-out. The large volume of these print-outs makes their repetition here impossible)

ϕ'_c (upper-bound) $= 2{,}914$

$s_n = 0{,}632$

$s_0 = 1{,}0$

$\delta = (\quad 1{,}0 - 0{,}632)$

$= 0{,}0368$

and ϕ'_c (lower-bound) $= 2{,}914 - 0{,}0368$

$= 2{,}887$

Approximate percentage error

$$= \pm \frac{0{,}5\ 0{,}0368}{0{,}5\ (2{,}914 + 2{,}887)}\ 100$$

$= \pm\ 0{,}6$

(3) $\Delta\phi = 0{,}01$: ϕ prism $= 4{,}0$

ϕ'_c (upper-bound) $= 2{,}901$

$s_n = 0{,}632$

$s_0 = 1,0$

$\delta = 0,01\ (1,0 - 0,632)$

$= 0,00368$

and ϕ'_c (lower-bound) $= 2,897$

Approximate percentage error $\simeq + 0,06$

i.e. provided $\Delta\phi_{ct}$ is small enough, the difference between upper and lower-bound solutions is negligible.

All subsequent calculations use a $\Delta\phi_{ct}$ value of 0,01. A low value is used because the calculations are computer processed. From the above assessment it is evident that a much higher value could have been used without a significant reduction in accuracy.

The variation of ϕ'_{ct} with x_i is examined in Table 3.2. It is evident that the magnitude of x_i has some impact on the result and must be taken into account in calculations.

Table 3.2 ϕ'_{ct} calculated for different x_i values ($\Delta\phi_{ct} = 0,01$)

x_i	Measured prism creep coefficient ϕ_{ct}					
	1	2	3	4	5	6
0,2	0,795	1,409	1,947	2,441	2,905	3,348
0,3	0,826	1,497	2,103	2,671	3,215	3,741
0,4	0,856	1,583	2,257	2,901	3,524	4,134
0,5	0,886	1,668	2,408	3,124	3,825	4,515
0,6	0,913	1,748	2,551	3,336	4,110	4,876

In Figure 3.2 ϕ'_{ct} is plotted against ϕ_{ct} for different values of x_i. Using these curves the calculation of long term deflection (excluding shrinkage) is reduced to a simple procedure:

(1) Calculate x_i and Δ_i for the completely cracked section.

(2) Determine ϕ_{ct} (prism) by direct measurement or by a proven calculation method for the concrete mix used in beam manufacture.

(3) From x_i and ϕ_{ct} determine ϕ'_{ct} using the curves of Figure 3.2. (Interpolate between x_i values where appropriate. The curves are approximately equally spaced, so accurate interpolation is possible).

(4) Then $\Delta_t = (1 + x_i . \phi'_{ct}) \Delta_i$. (3.15)

In conclusion, several points should be noted regarding the application of the above method.

This calculation method has been derived from the completely cracked section properties and should only be applied to concrete sections which are at least partially cracked under initial loading. This limitation is not as serious as it first appears as deflections are unlikely to be critical in substantially uncracked sections.

Shrinkage has not been considered in this evaluation. As noted in the introductory chapter, shrinkage affects

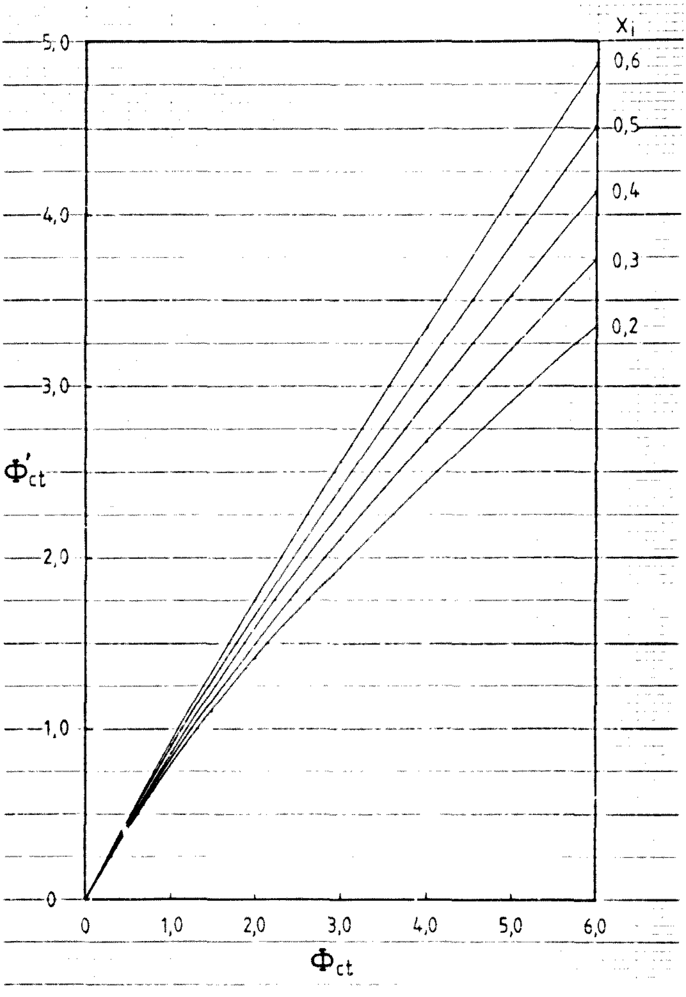

Figure 3.2 Φ'_{ct} versus Φ_{ct} (prism) for different x_i values

should be separated from *those of creep* if the coefficient approach is used in long term deflection calculation. Shrinkage deflection must be calculated independently of creep deflection if the method *derived* above is used.

This calculation method has been derived for singly *reinforced* (i.e. tension reinforcement only) rectangular beams. For sections containing compression reinforcement it may be possible to modify the calculation method. ϕ_{ct} *(prism)* could be factored by Branson's coefficient[8] $(1/(1 + 50\rho'))$ - experimentally derived) and the reduced value used to derive ϕ'_{ct} from Figure 3.2. Then Δ_t can be determined using *equation* 3.15.

The use of Branson's coefficient requires substantation by comparison with experimental results.

4. LABORATORY PROGRAMME

A proposed method of long term deflection calculation has been presented in Chapter 3. This method is based on a theoretically derived creep-dependent strain development across the beam depth. The specific objective of the laboratory programme is to provide experimental data for comparison with the proposed calculation method. It is necessary not only to compare measured and calculated deflections, but also to verify the theory upon which the calculation method is based.

The tests performed may be divided into two categories:

1) **Measurement of material properties required for long term deflection calculation.**

   Cube strength, elastic modulus, free shrinkage strain and creep strain were measured on concrete "control" prisms. Concrete tensile strength (modulus of rupture) was not measured. Where this parameter is required in deflection calculations a method of calculation (from compressive strength) is generally prescribed.

   It was not deemed necessary to verify the deflection related properties of the steel reinforcement by tests. All test beams were reinforced with high yield bars with a nominal yield strength of 450 MPa. A value of 210 GPa is used in all calculations for the elastic modulus of the reinforcement.

2) **Measurement of midspan strains and deflections on test beams.**

Shrinkage strains were measured on a single pre-cracked singly reinforced beam (Mk AW). Shrinkage deflections are calculated from these measured strains.

Long term deflections and midspan strains under sustained loading were monitored on four reinforced concrete beams, two containing tension reinforcement only (Mk A1 and A2) and two containing both tension and compression reinforcement (Mk B1 and B2).

4.1 TEST SPECIMENS

All test specimens were made from the same mix design. Mixing was undertaken on two separate occasions and the specimens from each mix are identified as Mk A and Mk B respectively. Control specimens for the measurement of concrete properties relevant to long term deflection calculation included:

(1) Twelve 4 inch cubes for compressive strength tests. *Three from each mix were crushed at 7 and 28 days.*

(2) Six (three from each mix) 200 x 100 x 100 mm prisms for the measurement of free shrinkage strain.

(3) Twelve (six from each mix) 200 x 100 x 100 mm prisms for the measurement of elastic modulus (Measurements were made at 28 and 210 days).

(4) Twelve (six from each mix) 200 x 100 x 100 mm prisms for the monitoring of creep strain.

Five reinforced concrete beams were constructed. Four 2200 mm long beams were used in the deflection tests under sustained load and one 1500 mm long beam was used for the monitoring of shrinkage strains at mid-span and the subsequent calculation of shrinkage deflection. Because of warp in the timber forms it has been necessary to base calculations on the actual beam dimensions rather than the nominal cross-sectional dimensions of 100mm x 150mm. Actual beam dimensions are derived by averaging measurements at midspan and at 400mm on either side of midspan. Beam cross-sections are shown in Figure 4.1

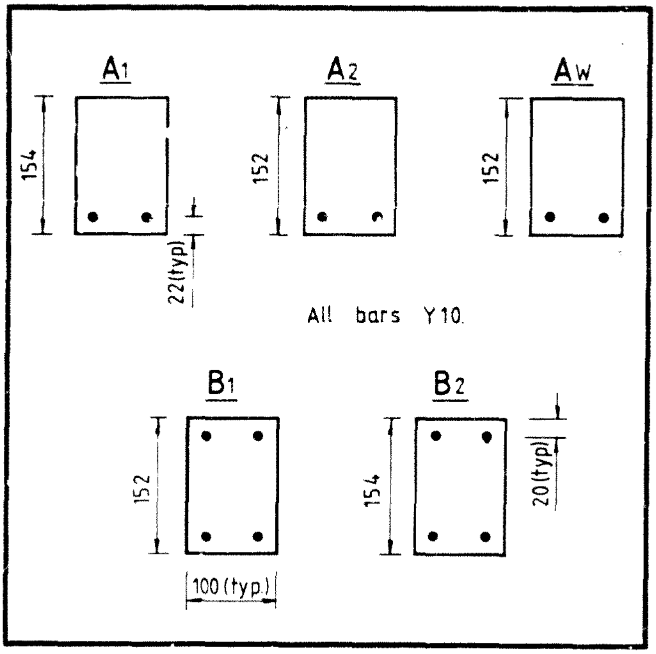

Figure 4.1 Test beam details

4.2 DETAILS OF MANUFACTURE

A normal weight concrete mix with a 28 day design characteristic cube strength of 25 MPa was used in the manufacture of all specimens. An above average water content was required to achieve suitable workability. Mix design details are given in Table 4.1. Mixing was undertaken on two separate occasions (18-06-85 and 24-06-85) and on each occasion 3 batches were mixed in a 100 litre pan mixer. Cubes and prisms were cast in steel moulds and the beams in timber forms. All specimens were mechanically vibrated. After the forms were stripped it became evident that a slight grout loss had occured in both beams and prisms at the joints in the forms. This was probably due to a shortage of fines in the sand. A concrete slump of 35mm was measured in the single test performed.

Table 4.1 Mix constituents

OPC ex Anglo Alpha, Roodepoort.	395 kg/m^3
Weathered granite pit sand	966 kg/m^3
12mm crushed quartzite - ex Hippo Quarries, East Rand	750 kg/m^3
Water	236 l/m^3
Cement/water ratio	1,67

Prisms and cubes were removed from their moulds after 24 hours. Beam side forms were stripped after 48 hours. All specimens were cured for a period of 28 days from the date of manufacture, the control specimens in a water bath at a temperature of 22°C and the beams under wet hessian and plastic sheets. (Temperature was not

ure 4.2 Location of demec targets on beams and prisms

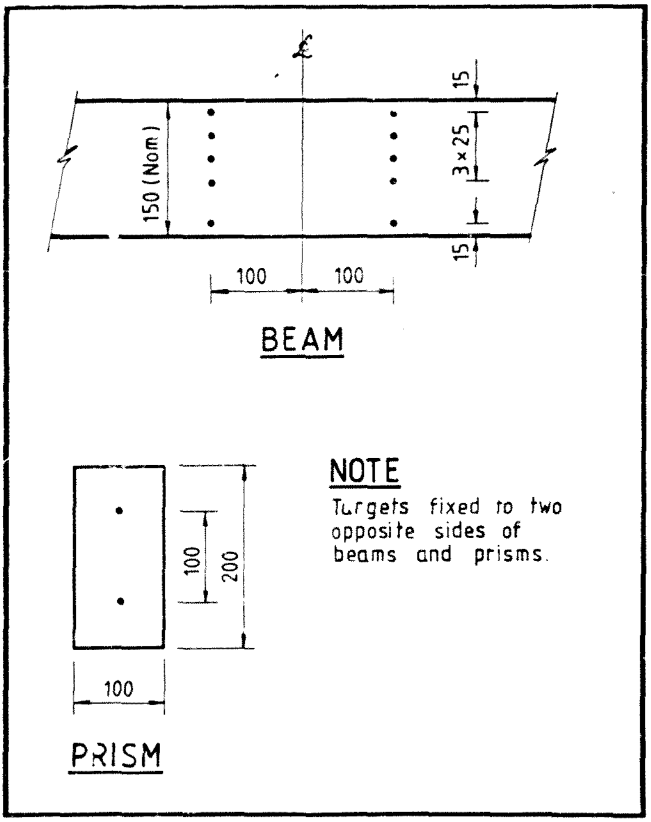

controlled during beam curing, but varied between about 10°C and 25°C).

During curing aluminium targets were glued to the prisms and beams for subsequent strain measurements using a demountable mechanical (DEMEC) strain gauge. The location of the targets is shown in Figure 4.2 for both the beams and prisms.

4.3 TEST PROCEDURE

4.3.1 CONTROL PRISMS

Cubes were crushed in compressive strength tests in accordance with SABS Method 863[15] at 7 and 28 days after manufacture. Three cubes from each mix were crushed on each occasion.

Elastic modulus was measured in a creep frame over a stress range of 9 MPa at 28 and 210 days. The 28 day test was performed on wet prisms and the 210 day test on dry prisms which had been stored in the same environment as the creep and shrinkage prisms. Six prisms from each mix were tested on each occasion. The same prisms were used in the two tests.

The opposite ends of the shrinkage prisms were wax sealed on completion of curing to simulate the exposure conditions of the creep specimens. Creep prisms were loaded to a stress of 10 MPa (approximately one third of compressive strength) in the creep frames (see Figure 4.3).

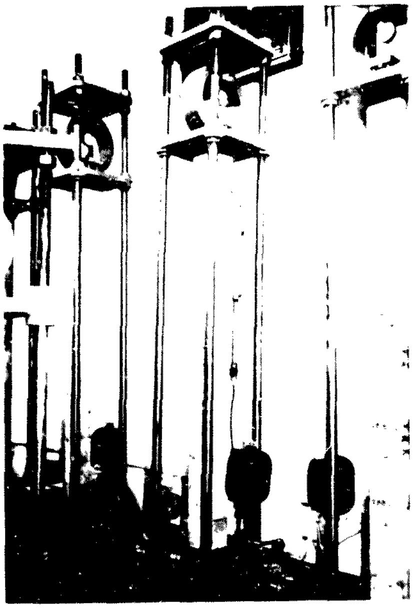

Figure 4.3 Prisms under load in creep frames

Six prisms were loaded in each creep frame. The creep frames were hydraulically loaded using flat jacks. The creep and shrinkage prisms were stored in a controlled environment at a temperature of 22°C and relative humidity of 60%.

4.3.2 TEST BEAMS

The four 2200 mm long beams were tested in a single steel frame. This arrangement is shown in Figure 4.4. Loads were applied horizontally by hydraulic jacks. The beams of each pair (Mk A and Mk B) were loaded against each other as shown in the photograph of Figure 4.5.

The horizontal orientation of the beams eliminated self-weight effects from deflection measurements.

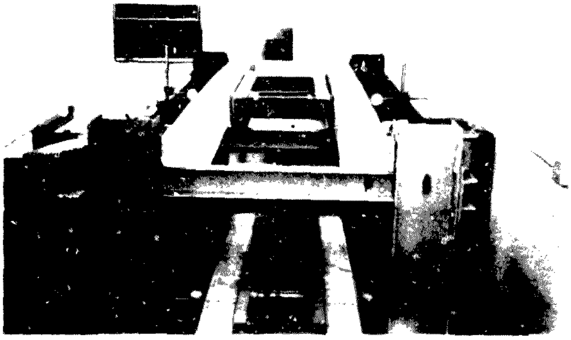

Figure 4 4 Arrangement of beams under load in test frame

A single load cell in series with each hydraulic jack was used to measure the applied load via a Huggenberger strain tester. The load from the jack was applied to a steel channel and from the channel as a third point load to the beam. A 10 mm wide masonite strip was inserted between the channel and the beam to prevent localised crushing of the concrete. The beam ends were supported on a 16 mm thick steel plate bearing on to a 20 mm diameter steel rod to simulate knife edge support conditions (see Figure 4 6). Midspan [illegible] were measured by dial gauges marked in [illegible] .01 mm. Both the jack loads and the loads applied in the creep frames had to be adjusted periodically to counter the effects of creep and pressure losses in the hydraulic systems.

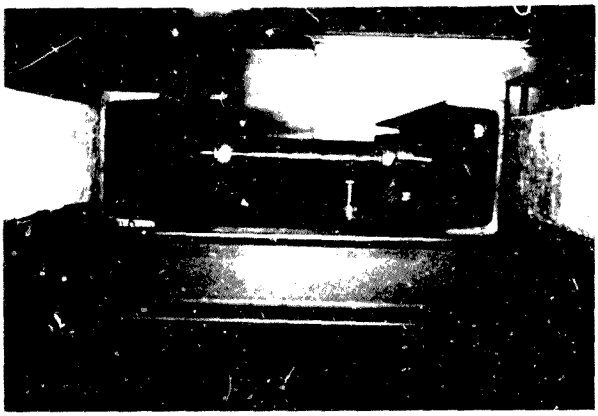

Figure 4.5 Details of method of load application

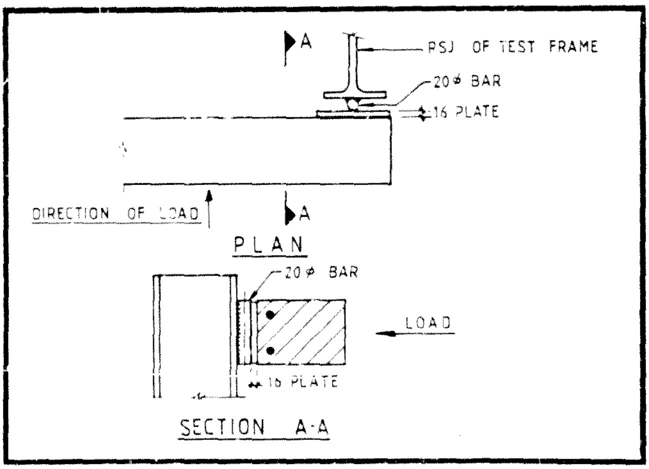

Figure 4.6 Support detail of beams under long term load

A load of 10 kN was applied by each jack. This resulted in a maximum applied moment of 3,5 kNm. The load arrangement is shown in Figure 4.7. The design ultimate moment (CP110) for the singly reinforced beams is approximately 6,0 kNm. This reduces to a moment of 3,8 kNm at working stresses by dividing by a live load factor of 1,6. A transverse (vertical) moment of 0,20 KNm was induced by the beam self weight. The effect of this moment on strains is deemed negligible as midspan strains are averaged from readings taken on both faces along the beam depth.

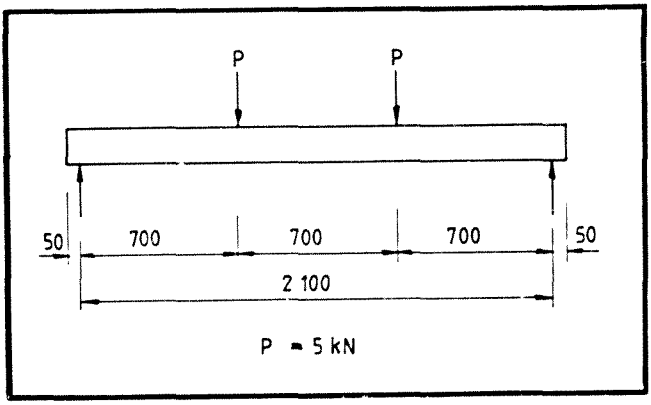

Figure 4.7 Beam Loading

The beam used for the measurement of shrinkage strains (Mk AW) was supported at its ends on a bearing plate and bar arrangement. This arrangement is shown in Figure 4.8. Note that beam Mk AW was supported horizontally as were the beams in the test frame. No deflection measurements were made on this beam. Deflections are calculated from measured strains.

All beams were stored in an environment of "controlled" temperature (approximately 22°C) but variable relative humidity. No continuous record was kept of relative humidity, but from periodic measurements made it appeared to vary between 35% and 60% depending on prevailing weather conditions. By far the greatest proportion of creep and shrinkage occurred during the dry winter months and an "average" relative humidity of 40% is used in all calculations. Creep and shrinkage measurements made on control prisms are adjusted for relative humidity and specimen size in deflection calculations (See Chapter 5 and Appendix D).

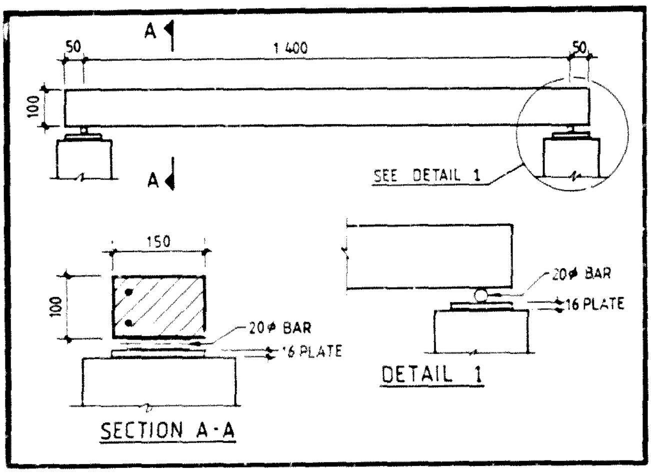

Figure 4.8 Support detail of shrinkage beam Mk AW

4.4 MEASUREMENTS

Each set of measurements consisted of strain measurements on creep and shrinkage prisms, deflection measurements on beams under sustained loading and midspan strain measurements on all beams. All loads were applied at 28 days on completion of curing. A set of measurements was taken immediately after loading, after three hours, daily for one week, weekly for one month and monthly thereafter up to six months after the end of curing.

5. TEST RESULTS

Test results are tabulated in appendices A to D. In order to limit the quantity of data presented, measurements made in the first month are not reported here.

5.1 CONTROL PRISMS

It is not the objective of this study to evaluate different methods of predicting the concrete properties required for long term deflection calculation. However, these properties had to be measured for deflection calculation and some comparison with expected or predicted values is required to ensure that the concrete mix used exhibits no anomalies which may give a bias to any conclusions drawn.

5.1.1 COMPRESSIVE STRENGTH AND ELASTIC MODULUS

Average results for concrete compressive strength and elastic modulus are given in *Table 5.1*. *Time* refers to time in days after manufacture and should not be confused with the time after loading or time after end of curing in creep and shrinkage tests respectively. It is clear that no benefit can be derived by considering different properties for the two mixes, and it is therefore proposed to use an elastic modulus (28 day value) of 21,5 GPa and a 28 day compressive strength of 32,4 MPa in all subsequent calculations. Where concrete cylinder strength is used in calculations its value is assumed to be 80% of the cube strength (Neville [16]).

Table 5.1 Concrete Properties

Concrete Props.	Compressive Strength (MPa)		Elastic Modulus (GPa)	
days	7	28	28	210
Mix:				
A	19,94	32,20	21,0	27,7
B	19,98	32,61	22,0	27,5

Davis[17] has investigated the rate of increase of cube strength for South African concretes made of Ordinary Portland Cement. A value of 0,70 was measured by Davis for f_7/f_{28} as compared with an average value of 0,62 from Table 5.1 above.

Elastic modulus values are considerably lower than those predicted by various methods as listed in Table 5.2. All predicted values are calculated from the measured compressive strength of 32,4 MPa at 28 days.

Table 5.2 Measured and predicted values of modulus of elasticity (All values in GPa)

E_c	PREDICTED			
Measured	CP110[1]	ACI 209[18]	Davis [17]	CEB 1978[19]
21,5	28,7	25,1	27,9	28,1

The low measured value of elastic modulus is not altogether unexpected. Alexander[20] has noted that weathered granite pit sand generally produces concrete exhibiting a high water demand and low 28 day modulus, and certain quartzitic coarse aggregates have been found by Davis[17] and others to yield low concrete elastic moduli.

The rate of increase of elastic modulus with time appears abnormally high. From the Cement and Concrete Association Development Report 3[11],

$$E_t = E_{28}(0{,}4 + 0{,}6\ f_t/f_{28}) \qquad (5.1)$$

which gives a predicted modulus (using a "typical" value of 1,15 for f_t/f_{28}) of 23,4 GPa at 210 days. Contrary to common practice, the 210 day test was performed on dry prisms. The high elastic modulus values probably result from the increased concrete strength accompanying drying.

Since elastic modulus varies with time, the selection of an E value for use in calculations poses a problem. It appears logical to use the value of E at the time of loading in immediate deflection calculations and this approach is adopted by codes. However, code recommendations vary for long term deflection calculation. CP110 makes no specific allowance for the variation in E but appears to advocate the use of the value applicable at the time of loading. A similar approach is adopted by ACI 318-83. CEB-FIP 1978[19] relates creep strain to the 28 day E value. The former approaches (CP110, ACI) are preferred as a measured creep coefficient will have an inherent correction for changes in E after the application of load. In this investigation the problem is eliminated by the application of loads at 28 days.

5.1.2 SHRINKAGE

Measured shrinkage strains are tabulated in Appendix A. Because the prisms were stored in a different environment (relative humidity) to the beams, and the volume/surface ratio of the prisms is different to that of the beams, it is necessary to modify the measured creep and shrinkage characteristics for the calculation of beam deflections. The recommendations of ACI Committee 209[18] are used for the modification as they deal with these effects individually and by equations (rather than charts) which are suitable for computer applications. The relevant equations are repeated below for reference.

$$\gamma_{vs} = 1,2e^{-0,00472\ v/s} \qquad (5.2)$$

where γ_{vs} is the volume/surface adjustment factor for shrinkage, and v/s is the volume/surface ratio in mm.

$$\gamma_{\lambda} = 1,40 - 0,010\lambda \quad \text{for } 40 \leq \lambda \leq 80 \qquad (5.3)$$

$$\text{or} \quad \gamma_{\lambda} = 3,00 - 0,030\lambda \quad \text{for } 80 \leq \lambda \leq 100 \qquad (5.4)$$

where γ_{λ} is the relative humidity adjustment factor for shrinkage and λ is the relative humidity in percent.

Free shrinkage strain calculated by various methods is compared with measured shrinkage strain in Table 5.3. The values listed in the table under "measured" are the averages for the six shrinkage prisms (three from each mix). Strain gauge measurements were made on two opposite faces of each prism, so that each strain value quoted represents the average of twelve measurements. Time refers to the time elapsed since the end of curing in this table. Values are not given where results are

Table 5.3 Calculated and measured free shrinkage (in units of microstrain)

Time (days)	28	60	90	120	180
ACI 209	251	342	391	420	454
CEB 1970[22]	360	446	498	531	550
CEB 1978	215	278	314	327	359
C & CA3	-	-	-	-	325
Measured (Average)	316	474	538	538	619

too close to be effectively separated in reading from curves. The validity of the C&CA 3 result is doubtful as its derivation requires considerable extrapolation.

The measured shrinkage strain is underpredicted by the calculation methods used. The mix used undoubtedly exhibits high shrinkage, but considerable scatter of measured results about the norm is generally expected[16]. It has also been noted by Neville[16] that concrete made with granite aggregate may exhibit above average shrinkage. In extensive tests Alexander[21] has found that the CEB-FIP (1978) method gives good results for South African concretes. Bakoss et al[7] maintain that the higher predictions of the ACI 209 recommendations give better results for Australian concretes. The discrepancy between the measured and calculated values emphasizes the importance of making preliminary measurements of concrete properties for deflection sensitive structures.

Shrinkage is expressed as a fraction of the 28 day shrinkage in Figure 5.1. From the curves it is evident that the rate of increase of shrinkage strain can be more accurately predicted than the ultimate shrinkage strain. Ultimate shrinkage should be predicted from short term tests where deflections are critical.

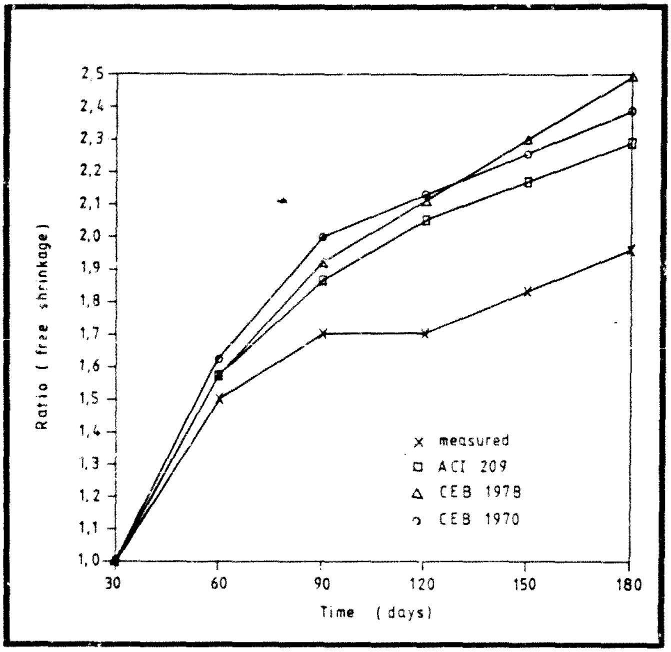

Figure 5.1 Measured and calculated rate of shrinkage (expressed as a fraction of 28 day shrinkage)

5.1.3 CREEP

Measured creep strains are tabulated in Appendix A. Again the measured results have to be modified for relative humidity and specimen size (by ACI 209 recommendations) for application in beam deflection calculations. The modifying equations are repeated below.

$$\tau_{vs} = 0{,}67(1 + 1{,}13e^{(-0{,}0213v/s)}) \quad (5.5)$$

$$\tau_{\lambda} = 1{,}27 - 0{,}0067\lambda \qquad \lambda > 40 \quad (5.6)$$

Total strain (shrinkage and creep) was measured on each prism. Creep strain is calculated by deducting measured shrinkage strain from the total strain value. Then, creep coefficient ("measured") = creep strain / initial strain,

$$\text{or } \phi_c = \frac{\epsilon_{cr}}{\epsilon_i} \quad (5.7)$$

Calculated and "measured" creep coefficients are compared in Table 5.4. The measured values listed represent the averages for twelve creep prisms (six from each mix) loaded in two creep frames (six per frame). Strain measurements were made on two opposite faces of each prism so each creep coefficient value quoted is the average calculated from twenty-four readings.

Time refers to the duration of loading. Values are not given where results are too close to be effectively separated in reading from curves. The derivation of the C&CA 3 results requires considerable extrapolation. The measured results agree fairly closely with the findings of Alexander[23] for South African concretes. The C & CA3 and CEB 1978 methods give the closest correlation with ACI 209 underestimating and CEB 1970[22] grossly overestimating.

Table 5.4 Calculated and measured creep coefficient

Time (days)	28	60	90	120	180
ACI 209	0,75	0,95	1,06	1,13	1,22
CEB 1970	2,66	3,29	3,68	3,92	4,07
CEB 1978	0,89	1,22	1,50	-	1,84
C & CA3	1,32	-	-	-	1,94
Measured (Avarage)	1,18	1,45	1,68	1,85	2,03

Creep is expressed as a fraction of the 28 day value in Figure 5.2. The rate of increase in creep strain is most accurately predicted by the ACI 209 method. As a general principle it should be possible to obtain a more accurate estimate of concrete creep (and shrinkage) characteristics by extrapolation from short term measured values than by pure calculation.

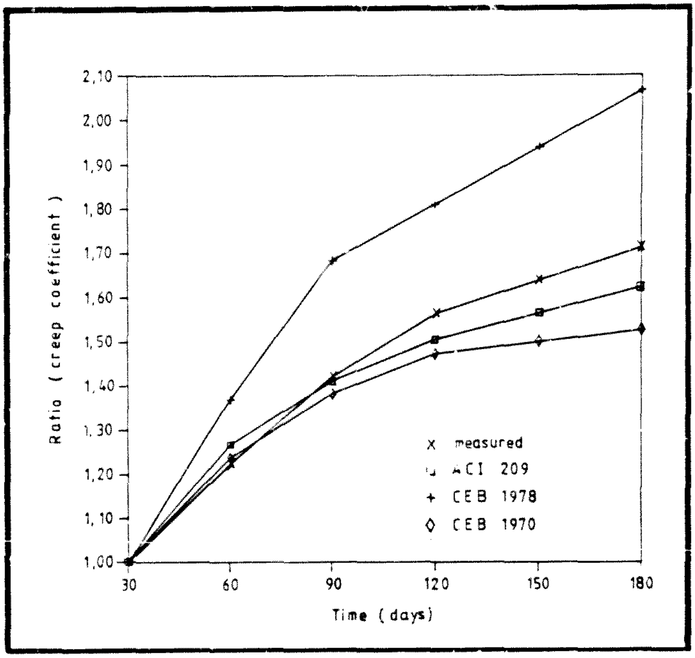

Figure 5.2 Measured and calculated rate of creep
(expressed as a fraction of 28 day creep)

5.2 BEAM MIDSPAN STRAINS

Strains measured across the beam depth are tabulated in Appendix B. Each value quoted is the average of two measurements made on the opposite faces of the beam. The location of the points of measurement is shown in

Figure 4.2. A detailed examination of the development of these strains with time is undertaken in this section for comparison with the theory on which the proposed calculation method (Chapter 3) is based.

5.2.1 STRAIN PROFILE

One of the few consistent conclusions in all the research results studied is that plane sections remain plane after the application of loads. This principle is confirmed by the results plotted in Figure 5.3. Total strains measured immediately after application of loads, after 28 days under load and after 180 days under load are shown in these diagrams. Only the shrinkage strains measured in beam Mk AW show a minor deviation from the straight line. As a result it is necessary to consider only extreme fibre compression strains and tensile strains at the level of the tension reinforcement in beam curvature calculations.

5.2.2 DEFLECTIONS CALCULATED FROM MIDSPAN STRAINS

Measured total deflections and deflections calculated from midspan strains are compared in Table 5.5. The calculated values vary between 87 and 100 % of the measured values. This is probably due to the erratic size and spacing of concrete tension cracks in the zone of measurement. The calculation procedure is outlined below.

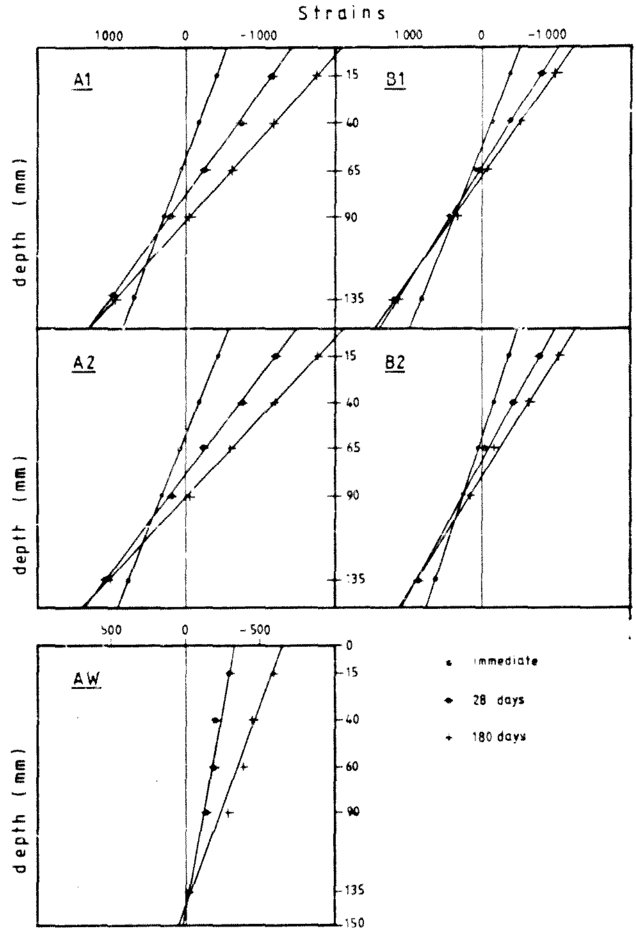

Figure 5.3 Measured total strains through beam section (in units of microstrain)

Table 5.5 Measured total deflections and deflections calculated from midspan strains

Time (days)			0	28	60	90	120	180
Mk	A1	Meas.	4,89	9,58	10,56	11,07	11,62	11,83
		Calc.	4,29	8,50	9,49	9,94	10,48	10,68
Mk	A2	Meas.	5,09	9,59	10,64	11,19	11,72	11,92
		Calc.	4,65	8,83	9,79	10,26	10,71	10,98
Mk	B1	Meas.	4,78	7,63	8,27	8,44	8,80	8,77
		Calc.	4,81	7,64	7,97	8,08	8,44	8,38
Mk	B2	Meas.	4,30	7,50	[illegible]	8,11	8,54	8,55
		Calc.	3,96	6,54	[illegible]	7,06	7,38	7,37

Curvature = $1/r = (\epsilon_s - \epsilon_c)/h$ (5.8)

Where ϵ_c = extreme compression fibre strain

and ϵ_s = extreme tension fibre strain

(h = 150 mm has been used in 5.8)

Deflection = $\Delta = k(1/r)\,l^2$ (5.9)

where k is a multiplying factor depending on the arrangement of applied loads.

5.2.3 SHRINKAGE STRAINS

Shrinkage strains across the depth of beam Mk AW have been measured for deduction from the total strains measured on beams Mk A1 and A2 and for the calculation of shrinkage deflections for those beams. Shrinkage strains were not monitored on the B series beams, so shrinkage deflections have to be calculated for those beams.

Beam Mk AW was initially loaded for a short period (approximately three minutes) to the same maximum moment as applied to the beams subjected to sustained loading in order to produce a cracking pattern similar to that exhibited by those beams. During the first few days of monitoring, strains in the opposite direction to the anticipated shrinkage strains were measured. This effect is attributed to a delayed recovery after the application of the short term load. In order to allow for this effect the three day strain measurements are taken as the zero value, and subsequent measurements are factored to cater for shrinkage deflection during the first three days. The factor is derived from the shrinkage strain measurements on unloaded prisms.

$$\text{Modification Factor} = F = \frac{\epsilon_{sht}}{\epsilon_{sht} - \epsilon_{sh3}} \qquad (5.10)$$

where ϵ_{sht} = prism shrinkage strain at time t and ϵ_{sh3} = prism shrinkage strain at 3 days. The legitimacy of this correction is illustrated in Figure 5.4 which shows the similarity in the rates of shrinkage strain measured on the control prisms and modified shrinkage deflection as measured on beam Mk AW.

The scales chosen for deflection and strain in Figure 5.4 are arbitrary. The s ty in their respective rates of development ited by the parallel nature of the curves.

Modified shrinkage deflection is calculated as follows:

$$(1/r)_{sh} = F \cdot \frac{\epsilon_c + \epsilon_s}{h} \qquad (5.11)$$

$$\Delta_{sh} = k \cdot (1/r)_{sh} \cdot l^2 \qquad (5.12)$$

where $k = 0,125$

(The "bending moment" caused by shrinkage is constant for a constant section along the beam length. $k = 0,125$ is the calculation factor for a constant moment along the length of the beam - refer Chapter 2, section 1).

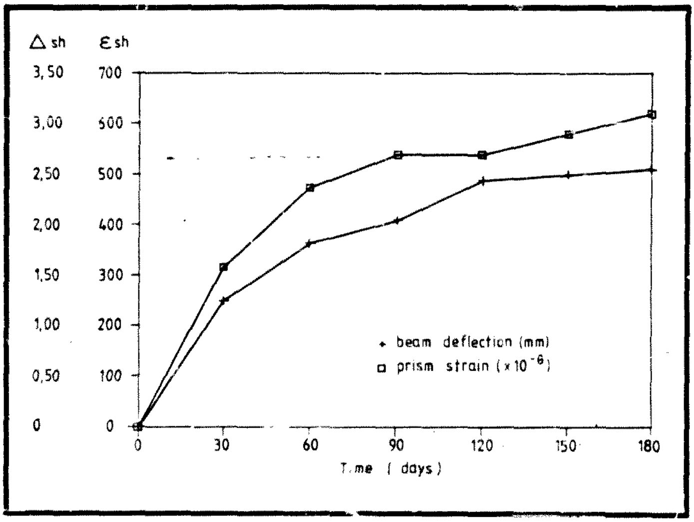

Figure 5.4 Comparison of shrinkage strain on control prisms and modified shrinkage deflection on beam Mk AW

Measured shrinkage strains (modified as described above) through the beam section are tabulated in Appendix B1. Extreme fibre strains with shrinkage deducted are tabulated in Appendix B2 fo beams A1 and A2.

5.2.4 STRAIN DEVELOPMENT IN EXTREME COMPRESSION FIBRE

In Chapter 3 it was theoretically shown that the creep coefficient in the extreme compression fibre is somewhat less than that measured on axially loaded prisms made of the same concrete. A method was derived (using the charts of Figure 3.2) for calculating the reduced coefficient.

Extreme compression fibre creep strains for the singly reinforced beams are recorded in Table 5.6. Shrinkage strains have been deducted from the given values (refer Appendix B2) From these a creep coefficient (creep strain divided by initial strain) for the extreme compression fibre is calculated and compared with the creep coefficient from Figure 3.2.

For both A1 and A2 the measured beam extreme fibre creep efficient is slightly less than that derived from jure 3.2, especially at 120 and 180 days. The correlation is good, however, when viewed in relation to the normal scatter exhibited by creep and shrinkage results The measured beam coefficients also very clearly show the decreasing trend (as compared with prism coefficients) with ime as predicted by calculation

One of the assumptions which the proposed calculation method is base hat the initial extreme fibre compression strain i el to that calculated by

Table 5.6 Comparison of extreme fibre creep with creep of control prisms (Creep is measured in units of microstrain)

Time (days)	28	60	90	120	180
<u>Mk. A1</u> ϵ_{ci} beam = 549 x_i = 0,380					
1. ϵ_{cr} beam	581	699	760	804	911
2. ϕ_c prism	1,307	1,599	1,859	2,053	2,255
3. ϕ_c beam (measured)	1,058	1,273	1,384	1,465	1,659
4. ϕ'_{ct} (Fig. 3.2)	1,07	1,27	1,45	1,59	1,73
<u>Mk. A2</u> ϵ_{ci} beam = 573 x_i = 0,382					
1. ϵ_{cr} beam	587	693	754	791	897
2. ϕ_c prism	1,307	1,599	1,859	2,053	2,255
3. ϕ_c beam (measured)	1,024	1,209	1,316	1,381	1,565
4. ϕ'_{ct} (Fig. 3.2)	1,07	1,27	1,45	1,59	1,73

elastic analysis assuming a fully cracked beam section. Calculated and measured values are compared in Table 5.7. A reasonable correlation is exhibited.

Table 5.7 Calculated and measured initial extreme fibre compression strains (in units of microstrain)

Ext. fibre compression strain	Beam Mk			
	A1	A2	B1	B2
Calculated	563	577	468	456
easured	549	573	554	511

5.2.5 STRAIN DEVELOPMENT AT LEVEL OF TENSION REINFORCEMENT

Strains at the level of the tension reinforcement were assumed to remain constant and equal to the values calculated assuming a completely cracked beam section in the derivation of the proposed calculation method. This assumption was based on the observation that these strains increase very rapidly to a limiting value in beams subjected to sustained loading.

Measured strains at beam midspan are tabulated in Appendices B1 (total strain for all beams) and B2 (extreme fibre strains with shrinkage deducted for beams MK A1 and A2). Strains at the level of the tension reinforcement are calculated from extreme fibre strains as follows:

$$^1/_r = \frac{\epsilon_c + \epsilon_t}{h} \qquad (5.13)$$

where ϵ_c = extreme fibre compression strain

ϵ_t = extreme fibre tension strain

then $\epsilon_s = \epsilon_t - (1/r)\,(h - d) \qquad (5.14)$

where ϵ_s = strain at level of tension reinforcement.

Measured h values (i.e. h = 154 for A1 and B2, h = 152 for A2 and B1) have been used in these calculations.

Strains thus calculated are listed in Table 5.8. These strains show a marked increase in the first month under load (approximately 40 %) and thereafter remain fairly constant. Shrinkage strains have been deducted from the strain values quoted for beams A1 and A2 but not for beams B1 and B2. The higher values of $\epsilon_{st}/\epsilon_{si}$ calculated for beams A1 and A2 result from this. Typical strain distributions for the loaded and unloaded beams are shown in Figure 5.5. If sketch (i) represents the total strain distribution and (ii) the shrinkage strain distribution, it is evident that deducting shrinkage results in an increased strain equal to $\epsilon_s + \epsilon_{sh}.(h - d)/d$ at reinforcement level.

Calculated initial strains from the completely cracked section are compared with measured strains in Table 5.9. Again the values quoted for A1 and A2 have shrinkage deducted while those for B1 and B2 do not.

Table 5.8 Measured strains at level of tension reinforcement (in units of microstrain)

Beam Mk	Time (days)					
	0	28	60	90	120	180
A1						
ϵ_s	625	913	932	936	921	883
$\epsilon_{st}/\epsilon_{si}$	1,00	1,46	1,42	1,50	1,47	1,41
A2						
ϵ_s	698	967	991	998	968	[illegible]
$\epsilon_{st}/\epsilon_{si}$	1,00	1,39	1,42	1,43	1,39	1,36
B1						
ϵ_s	760	1035	1023	989	1060	1049
$\epsilon_{st}/\epsilon_{si}$	1,00	1,36	1,35	1,30	1,39	1,38
B2						
ϵ_s	574	782	766	736	787	771
$\epsilon_{st}/\epsilon_{si}$	1,00	1,36	1,33	1,28	1,37	1,34

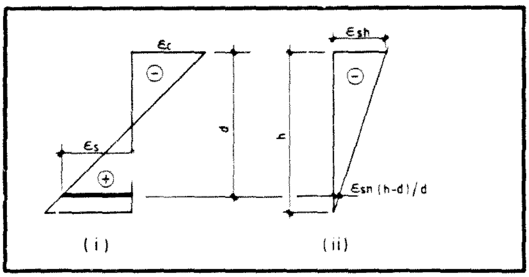

Figure 5.5 Typical strain distribution through sections of loaded (i) and unloaded (ii) beams

As can be expected, the calculated *initial* strains are considerably higher than measured *initial* strains because calculations are based on the completely cracked section. Strains thus calculated agree closely with the measured long term strains. This appears to indicate that the completely cracked condition was reached soon after the application of loads.

Table 5.9 Calculated and measured strains at level of tension reinforcement (in units of microstrain)

Beam Mk	A1	A2	B1	B2
ϵ_{si} (calc.)	920	935	906	891
ϵ_{si} (meas.)	625	698	760	574
ϵ_{s180}(meas)	883	950	1049	771

5.3 BEAM DEFLECTIONS

5.3.1 SHRINKAGE DEFLECTIONS

Shrinkage deflections were not measured directly on beam Mk AW. Deflections are calculated from strains measured at beam midspan. The calculation method and application of a modification factor to cater for delayed creep recovery are described in 5.2.2. Beams Mk A1 and A2 are essentially identical to AW in cross-section and shrinkage deflections for A1 and A2 can be readily calculated from equation (5.1), $\Delta_{sh} = k(1/r).l^2$, by considering $l = 2100$ mm. Deflections calculated from measured midspan strains are tabulated in Appendix D1, and for purposes of comparison are considered to be "measured" deflections.

A comprehensive comparison o[illegible]thods of shrinkage deflection calculation has undertaken by Hobbs[24]. He concludes that sh[illegible] deflections can be calculated most accurately by [illegible] equivalent tensile force (ETF) method.

Shrinkage deflection "measured" on beam Mk AW and adjusted for the 2100 mm long beams is compared with values calculated by the ETF method and CP110 in Table 5.10. The former method makes specific allowance for the cracked section while the latter does not. The measured values compare very favourably with those calculated by CP110, but are significantly overestimated by the ETF method. This is probably due to the fact that the section is only partially cracked, although a better correlation might be expected.

The ETF method includes terms catering for creep and a correspondingly reduced EI value (modular ratio calculation). Some doubt exists as to the creep value to be used in calculations. Hobbs suggests that for small concrete sections a value one month after drying begins and for larger sections a value one year after drying begins should be used in the calculation of ultimate shrinkage deflection. The values of Table 5.10 have been calculated using 0,3 times the measured creep coefficient at time t.

Table 5.10 Measured and calculated shrinkage deflection (in mm) for beams Mk A1 and A2.

Time after curing (days)	28	60	90	120	180
Measured	1,25	1,82	2,05	2.44	2,55
CP110	1,21	1,82	2,07	2.07	2,37
ETF	2,66	4,25	5,11	5,31	6,34

No shrinkage strain measurements were made for the doubly reinforced beams Mk B1 and B2. In view of the accuracy achieved in calculating shrinkage deflections for the singly reinforced beams using the method prescribed by CP110, the same method has been used to "estimate" shrinkage deflection for beams B1 and B2. The calculated deflections are listed in Table 5.11.

Table 5.11 Shrinkage deflections (*in mm*) for beams Mk B1 and B2 calculated by method of CP110

Time after curing (days)	28	60	90	120	180
Δ_{sh} (mm)	0,31	0,47	0,54	0,54	0,62

It must be emphasized that attention is primarily focussed on creep deflections in this *investigation*. Shrinkage measurements have been made to enable the deduction of this variable from the observed long term results. Unfortunately the concrete mix used exhibits high *shrinkage which* affects the accuracy of the creep results. In retrospect it would have been desirable to devote greater attention to shrinkage deflection. In particular, inaccuracies *are introduced* by the calculation of shrinkage deflections from measured strains and by the correction required for the initial creep recovery.

5.3.2 CREEP DEFLECTIONS

A method of long term deflection calculation (excluding shrinkage) was developed in Chapter 3. The assumptions and theory regarding the development with time of midspan strains across the beam depth were shown to be in good agreement with observed results in section 5.2. In this section deflections calculated by the proposed method are compared with measured deflections.

A description of some existing methods of long term deflection calculation was given in Chapter 2. Of the methods examined, those of CP110[1] and Neville[5] are specifically prescribed for the calculation of long term deflection due to creep only.

Measured long term deflections are compared with deflections calculated by the proposed method, CP110 and Neville's method in Table 5.12 and Figures 5.6. and 5.7. Shrinkage deflections have been deducted from the measured values quoted. For the A series beams shrinkage deflections were calculated from shrinkage strains measured on beam Mk AW. For the B series beams shrinkage deflections have been estimated using the calculation method prescribed by CP110 (refer section 5.3.1). Values of x_i in the table are quoted for information and are calculated from the fully cracked section. ϕ'_{ct} values are determined from Figure 3.2. The value of ϕ_{ct} quoted is calculated from prism strain measurements (Appendix A) and modified by ACI 209 recommendations for the different storage environment and volume/surface ratio of the beams.

The fact that the proposed calculation method is based on the initial strain distribution of the completely cracked section does not imply that the completely cracked section calculation is recommended for initial deflection calculation. It is essential to consider tension stiffening in initial deflection calculations. The fully cracked section initial deflection is given in brackets under the "proposed" method for information only.

Table 5.12 Calculated and measured long term deflections (shrinkage deducted)

Time (days)	0	28	60	90	120	180
A1						
x_1 = 0,380						
ϕ_{ct}	-	1,307	1,599	1,859	2,053	2,255
ϕ'_{ct}	-	1,07	1,27	1,45	1,59	1,73
Neville	4,78	6,56	6,96	7,32	7,57	7,85
CP110	4,59	6,54	6,93	7,27	7,53	7,80
Proposed	(5,28)	7,43	7,83	8,19	8,47	8,75
Measured	5,89	8,33	8,74	9,02	9,18	9,28
A2						
x_1 = 0,382						
ϕ_{ct}	-	1,307	1,599	1,859	2,053	2,255
ϕ'_{ct}	-	1,07	1,27	1,45	1,59	1,73
Neville	4,99	6,86	7,28	7,65	7,93	8,22
CP110	4,77	6,79	7,20	7,56	7,83	8,11
Proposed	(5,47)	7,71	8,12	8,50	8,79	9,08
Measured	5,09	8,34	8,82	9,14	9,28	9,37

Table 5.12 (Continued)

Time (days)	0	28	60	90	120	180
<u>B1</u>						
x_i = 0,341			ρ' = 0,012			
$\Phi_{ct}/(1+50\rho')$	-	0,817	0,999	1,162	1,283	1,409
Φ'_{ct}	-	0,70	0,83	0,93	1,03	1,13
Neville	4,49	5,33	5,52	5,69	5,81	5,95
CP110	4,39	5,42	5,57	5,70	5,80	5,89
Proposed	(5,10)	6,32	6,54	6,72	6,89	7,07
Measured	4,78	7,32	7,80	7,90	8,26	8,15
<u>B2</u>						
x_i = 0,339			ρ' = 0,012			
$\Phi_{ct}/(1+50\rho')$	-	0,817	0,999	1,162	1,283	1,409
Φ'_{ct}	-	0,70	0,83	0,93	1,03	1,13
Neville	4,30	5,09	5,27	5,43	5,55	5,67
CP110	4,23	5,21	5,36	5,49	5,58	5,67
Proposed	(4,93)	6,09	6,32	6,48	6,65	6,82
Measured	4,30	7,19	7,44	7,57	8,00	7,93

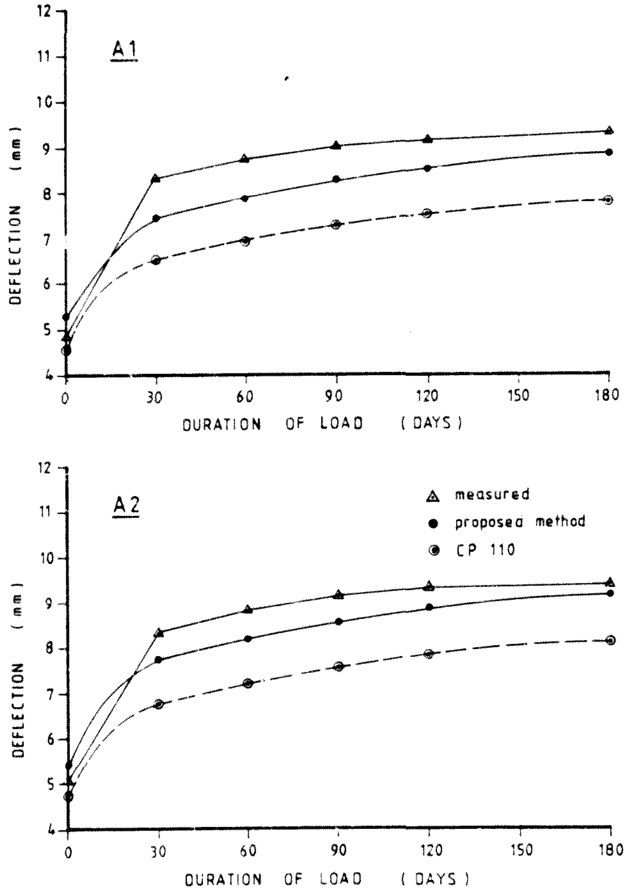

Figure 5.6 Measured and calculated long term deflections for beams A1 and A2 (shrinkage deducted)

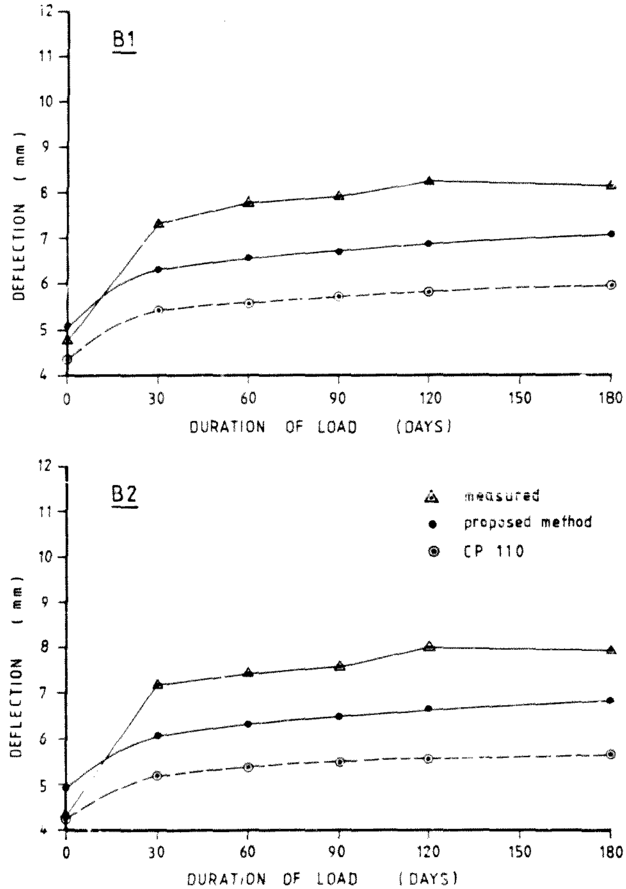

Figure 5.7 Measured and calculated long term deflections for beams B1 and B2 (shrinkage deducted)

All calculation methods underestimate measured deflections. The CP110 and Neville calculation methods give very similar results. For beams Mk A Δ calc./Δ meas. for the proposed method varies between 0,89 at 28 days and 0,97 at 180 days. This ratio varies between 0,79 at 28 days and 0,87 at 180 days for the CP110 method. For beams Mk B Δ calc./Δ meas. for the proposed method varies between 0,85 and 0,87 and for the CP110 method varies between 0,72 and 0,74. The relatively lower values calculated for the B series beams may result from an underestimation of shrinkage deflection for these beams by the method of CP110.

5.3.3 TOTAL DEFLECTIONS

It was noted in Chapter 1 that creep and shrinkage effects should be separated where possible if the coefficient approach is adopted for long term deflection calculation. It is acknowledged, however, that the separation of these effects is not always practical in comparing calculated and observed results (as for beams Mk B in this investigation) and is perhaps an unnecessary refinement if creep and shrinkage characteristics have not been measured on control prisms.

Total long term deflections are compared with deflections calculated by the method of the SAICE (Pretorius[6]) in Table 5.12. Δ calc./Δ meas varies between 0,89 at 28 days and 0,96 at 180 days for the series A beams, and between 0,84 at 28 days and 0,86 at 180 days for the series B beams. A very similar degree of accuracy was achieved using the proposed calculation method to predict long term deflection with shrinkage deducted (refer Table 5.12.)

Table 5.13 Calculated and measured total long term deflections (shrinkage included)

Time (days)	0	28	60	90	120	180
ϕ_{ct}	-	1,307	1,599	1,859	2,053	2,255
<u>A1</u>						
SAICE	(5,28)	8,57	9,32	9,98	10,48	11,00
Measured	4,89	9,58	10,56	11,07	11,62	11,83
<u>A2</u>.						
SAICE	(5,47)	8,89	9,87	10,36	10,88	11,42
Measured	5,09	9,59	10,64	11,19	11,72	11,92
<u>B1</u>.						
SAICE	(5,10)	6,53	6,86	7,15	7,36	7,58
Measured	4,78	7,63	8,27	8,44	8,80	8,77
<u>B2</u>.						
SAICE	(4,93)	6,30	6,61	6,89	7,10	7,31
Measured	4,30	7,50	7,91	8,11	8,54	8,55

6. RESEARCH RESULTS OF OTHER INVESTIGATORS

Three sets of results are examined in detail in this section. These are the results of Washa and Fluck[12], Corley and Sozen[13] and Bakoss et al[7], and have been selected from the vast body of research data for the following reasons:

1) Deflection measurements were made on rectangular beams with and without compression reinforcement.

2) Concrete creep and shrinkage characteristics were measured on control prisms.

3) Midspan strains were monitored.

4) Results are generally reported in sufficient detail in the references quoted to enable effective comparison with deflections calculated by the method of Chapter 3.

It was hoped that the hypotheses of Chapter 3 regarding creep strain development could be verified by comparison with the results of other researchers. This has not been possible. In all three references examined here measured strains are reported graphically on small scale curves and can only be read to an estimated accuracy of + 10%. The effect of the time lag between loading and initial reading reported by Washa and Fluck (see Section 6.1) is evident in their measured strains and makes their results difficult to interpret. Consequently, a rigorous quantitive comparison is only undertaken for measured and calculated deflections. The evaluation of strain development is limited to very brief comments on significant observations made

It will be noted that experimental error and inconcise or incomplete reporting very often make precise comparison difficult.

6.1 WASHA AND FLUCK [12]

Thirty-four beams were subjected to a uniformly distributed sustained load for a period of two and a half years. Only the results of series A and B beams are evaluated here. The results of series C, D, and E beams which were designed to represent thin reinforced slabs are not deemed particularly relevant because of the high span/d ratios. Essential beam details are listed in Table 6.1. Each result presented represents the average for two identical beams (e.g. the results listed under A1 4 are the averages for beams A1 and A4).

The authors report a significant time lapse (between one and eight hours) between the application of loads and the first readings, but do not elaborate on any effects this may have had on the results.

Initial deflections calculated from measured strains exceed measured deflections by approximately 30%. Initial measured compression strains exceed the values calculated assuming a fully cracked section by a similar amount. Both effects probably result from the time lag between loading and reading. It would appear that deflections were measured prior to strains. Because of this no effective evaluation of strain development can be undertaken.

Shrinkage and creep effects were not separated in beam series A and B. 12" x 4" x 4" prisms subjected to a sustained compressive stress of 11,08 MPa exhibited an

Table 6.1 Beam Details (Washa and Fluck)

Washa & Fluck	Beam Mk					
	A1/4	A2/5	A3/6	B1/4	B2/5	B3/6
<u>Beam Properties</u>						
b (mm)	203	203	203	152	152	152
d (mm)	257	257	257	157	157	157
h (mm)	305	305	305	203	203	203
d' (mm)	48	48	-	46	46	-
l (mm)	6096	6096	6096	6096	6096	6096
A_s (mm²)	855	855	855	396	396	396
As' (mm²)	855	396	0	396	198	0
ρ	0,0164	0,0164	0,0164	0,0164	0,0164	0,0164
ρ'	0,0164	0,0076	0	0,0164	0,0082	0
ρ_o (CP110)	0,178	0,487	0,822	0,178	0,457	0,822
<u>Loading</u> (UDL)						
w (KN/m)	5,63	5,63	5,63	1,59	1,59	1,59
M (KNm)	26,15	26,15	26,15	7,39	7,39	7,39
k	0,1042	0,1042	0,1042	0,1042	0,1042	0,1042
<u>Mix Characteristics</u>						
f_{cu} (MPa)	30	30	30	30	30	30
f_{meas} (MPa)	32,3	32,3	32,3	32,3	32,3	32,3
E_c (GPa)	21,7	21,7	21,7	21,7	21,7	21,7
$\phi_{c,sh}$ pris	6,54	6,54	6,54	6,54	6,54	6,54
ϕ_c pris	4,97	4,97	4,97	4,97	4,97	4,97
ϵ_{sh} pris	---------- 800.10^{-6} ----------------					

Table 6.2 Calculated and measured deflections (Washa and Fluck)

Washa & Fluck	Beam Mk					
	A1/4	A2/5	A3/6	B1/4	B2/5	B3/6
ϕ_c beam	3,91	3,91	3,91	4,32	4,32	4,32
$\phi_c/(1+50\rho')$	2,15	2,83	3,91	2,37	3,06	4,32
ϵ_{sh} beam	673	673	673	734	734	734
ϵ_{ci}	390	436	491	444	466	494
x_i	0,378	0,402	0,427	0,401	0,414	0,428
ϕ'_{ct} Fig 3.2	1,66	2,15	2,91	1,83	2,33	3,17
Δ_{sh}	2,2	5,9	10,0	3,9	9,9	17,9
<u>Immediate Deflection</u> (mm)						
CP110	13,7	14,3	15,1	22,2	22,6	23,1
Neville	13,8	14,7	15,6	22,2	22,9	23,9
Cracked	16,0	[illegible],6	17,4	27,7	28,1	28,5
Measured	13,5	15,7	17,0	23,4	24,9	26,4
<u>Long Term Deflection</u> (mm) (Shrinkage deducted)						
CP110	20,1	24,6	34,7	37,9	43,4	55,5
Neville	22,7	27,7	36,0	36,6	42,9	55,0
Proposed	26,0	30,9	39,0	48,0	55,2	67,2
Measured	21,4	26,4	34,7	47,2	55,1	68,5
<u>Long Term Deflection</u> (mm) (Shrinkage included)						
SAICE	31,0	42,0	53,8	58,0	75,5	94,9
Measured	23,6	32,3	44 7	51,1	65,0	86,4

Values quoted for ϵ_{sh} and ϵ_{ci} are in units of microstrain. Δ_{sh} has been calculated by the method of CP110.

additional long term strain of 3333.10^{-6}. Using an average modulus of elasticity (measured) of 21,73 GPa this gives an inital strain of 510.10^{-6} and a combined shrinkage and creep coefficient of 6,535. Shrinkage prisms exhibited a free shrinkage strain of 800.10^{-6} over the two and a half year duration of the test. This results in a "creep only" coefficient of 4,97.

Calculated and measured deflections are compared in Table 6.2. The creep coefficient and free shrinkage strain (ϕ_c and ϵ_{sh}) are adjusted (by ACI 209 recommendations) for the different volume/surface ratio of the beams. Only the adjusted values are shown in the table. Shrinkage deflections have been calculated by the method of CP 110 for deduction from total deflections.

6.2 CORLEY AND SOZEN[13]

Two equivalent point loads were applied at quarter points on three rectangular reinforced concrete beams for a duration of two years. The concrete shrinkage and creep characteristics were measured on 4" diameter cylinders. A single pre-cracked beam (C2) was used to measure shrinkage deflection. Beam details are listed in Table 6.3.

Deflections calculated from measured strains (initial and long term) are approximately 90% of the measured values. Measured compression strains are marginally lower than the values calculated assuming a fully cracked beam section. It is noted in reference (13) that measured strains at the level of the tension reinforcement were initially much lower than the values predicted for the fully cracked section, but reached the calculated value rapidly (within 10 days) and exceeded it by about 10% at the end of the test period.

Table 6.3 Beam details (Corley and Sozen)

Corley & Sozen	Beams Mk		
	C1, C2	C3	C4
Beam Properties			
b (mm)	76	76	76
d (mm)	137	92	92
h (mm)	153	110	110
l (mm)	1829	1829	1829
A_s (mm^2)	143	143	214
A_s' (mm^2)	-	-	-
ρ	0,0137	0,0205	0,0306
ρ'	-	-	-
ρ_o (CP110)	0,774	0,887	1,00
Loading (1/4 point)			
P (kN)	5,09	5,09	5,09
M (kNm)	2,32	2,32	2,32
k	0,1146	0,1146	0,1146
Mix Characteristics			
f_{cu} (MPa)	26,4	26,4	26,4
f_{meas} (MPa)	33,4	33,4	33,4
E_c (GPa)	21,1	21,1	21,1
ϕ_c (prism)	3,00	3,00	3,00
$\phi_{c,sh}$ (prism)	3,67	3,67	3,67
ϵ_{sh} (prism)	$300 \cdot 10^{-6}$	$300 \cdot 10^{-6}$	$300 \cdot 10^{-6}$

The results are generally reported graphically and inaccuracies may arise in reading from curves. It is stated in the text that free shrinkage and creep strain "approached" 300.10^{-6} and 1350.10^{-6} respectively at the end of the test period - in the absence of more accurate information these values have to be used in comparative calculations. The creep coefficient is reported to have "approached" 3,0.

Control cylinders for creep testing were subjected to a sustained stress of 9,5 MPa. From the approximate information given above an initial elastic modulus value of 21,1 GPa and total coefficient (shrinkage and creep) of 3,67 can be calculated.

Normally cylinder creep and shrinkage values have to be adjusted for use in deflection calculations because of the different volume/surface ratio of the beams. In this instance the volume surface ratio of the beams is very similar to that of the cylinders, so no adjustment is required.

Shrinkage deflections were measured on a single pre-cracked beam similar to C1. The measured value of 1,52 mm is 2,14 times the CP110 calculated value of 0,71 mm. Accordingly, for beams C3 and C4 the shrinkage deflection is estimated as 2,14 times the CP110 calculated value.

Measured and calculated deflections are compared in Table 6.4.

Table 6.4 Calculated and measured deflections (Corley and Sozen)

Corley & Sozen	Beams Mk		
	C1	C3	C4
ϕ_c beam	3,00	3,00	3,00
ϵ_{sh} beam	300.10^{-6}	300.10^{-6}	300.10^{-6}
ϵ_{ci}	441.10^{-6}	868.10^{-6}	779.10^{-6}
x_i	0,404	0,466	0,533
ϕ'_{ct} Fig 3.2	2,26	2,35	2,47
Δ_{sh} (est.)	1,5	2,6	2,9
<u>Immediate Deflection</u> (mm)			
CP110	2,7	7,2	5,7
Neville	2,7	7,6	6,0
Cracked	3,1	7,8	6,1
Measured	3,0	7,9	6,1
<u>Long Term Deflection</u> (mm) - Shrinkage deducted			
CP110	5,3	14,9	12,9
Neville	5,2	16,2	14,3
Proposed	5,9	16,3	14,1
Measured	5,9	14,7	12,6
<u>Long Term Deflection</u> (mm) - Shrinkage included			
SAICE	7,7	21,2	17,9
Measured	7,4	17,3	15,5

6.3 BAKOSS, GILBERT, FAULKES AND PULMANO[7]

One simply supported and one continuous beam were subjected to sustained loading for a duration of 500 days. Only the simply supported beam (1 B2) deflections are examined here. Two equal loads were applied at third points on this beam. Shrinkage deflection was monitored on a similar pre-cracked beam (1 B1). Beam details are given in *Table 6.5*.

Table 6.5 Beam details (Bakoss et al)

Beams Mk IB1 and IB2			
<u>Beam Properties</u>		<u>Loading (1/3 point)</u>	
b (mm)	100	P (kN)	2,60
d (mm)	130	M (kNm)	3,25
h (mm)	150	k	0,1065
l (mm)	3750		
A_s (mm²)	226		
As' (mm²)	-		
ρ	0,0174	<u>Mix Characteristics</u>	
ρ'	-		
ρ_o	0,838	f_{cu} (MPa)	37,5
		f_c meas. (MPa)	48,8
		E_c (GPa)	31,2
		ϕ_c	2,4
		ϵ_{sh}	$650 \; 10^{-6}$

Creep coefficient and free shrinkage strain are only reported for the mix used in the construction of the continuous beam. Both parameters were measured on 100 mm x 150 mm x 400 mm prisms. The mix used for the simply supported beam differs only marginally from this, and the two mixes are assumed to exhibit identical characteristics for calculation purposes.

Deflections calculated from measured midspan strains vary between 72% and 123% of the fully cracked section calculated value. The initial measured compression strain is considerably less than the cracked section calculated values. Strain measured at the level of the tension reinforcement increased by an estimated 63% over the duration of the test.

Calculated and measured deflections for beams 1 B1 and 1 B2 are compared in Table 6.6. The volume surface ratio of the prisms is the same as that of the beams, so no adjustment needs to be made to the creep and shrinkage parameters measured on prisms

Table 6.6 Calculated and measured deflections (Bakoss et al)

ϕ_c beam	2,4	ϵ_{sh} beam	650.10^{-6}
ϵ_{ci}	370.10^{-6}	ϕ'_{ct}	1,83
x_i	0,381		
Immediate Deflection (mm)		Shrinkage Deflection (mm)	
CP110	9,77	CP110	7,37
Neville	9,35	ETF	17,84
Cracked	11,22	Measured	6,94
Measured	8,94		
Long Term Deflection			
Shrinkage Deducted		Shrinkage Included	
CP110	17,10	SAICE	24,21
Neville	15,75	Measured	25,06
Proposed	19,04		
Measured	18,12		

7. EVALUATION OF RESULTS

Numerous comparisons have been made in Chapters 5 and 6 between observed results and the predictions of the calculation method developed in Chapter 3. Calculated and measured deflections compare very favourably, but strain results exhibit some scatter. This chapter is devoted to a consideration of possible explanations for some of the observed inconsistencies and a closer examination of the accuracy achieved in deflection prediction.

It is apparent that deflections cannot be accurately predicted from measured midspan strains. Some discrepancy between measured and calculated is expected because measured tensile strains are dependent on the spacing of the tension cracks in the concrete. Crack spacing tends to be erratic. Improved accuracy could be expected where the gauge length is much greater than the crack spacing. In the beams of this study tension cracks occured at approximately 50 mm intervals (i.e. four cracks over the 200 mm gauge length). In my opinion this should have been sufficient to provide an accurate average tensile strain measurement.

In both the observations of this investigation and those of Corley and Sozen(13) deflections calculated from measured strains are approximately 90% of the measured deflection values. Deflections could have been "over-measured" due to concrete crushing at the supports, but this was not evident in the beams tested in this investigation. Unfortunately I can offer no other logical explanation for this observation, but if measured strains do not accurately predict deflection, it cannot be expected that measured and calculated strains will exhibit good correlation.

Temperature changes can make a significant contribution to the scatter exhibited by strain results. Although temperature was controlled in the storage environment of this study, it actually varied by +- 2°C from the mean of 22°C. Bakoss et al[7] report a similar variation in the temperature of their "controlled" storage environment. To analyse the impact of such a variation, consider its possible effect on beam Mk A1.

Initial compression strain (*measured in extreme fibre*)

$$= \epsilon_{ci} = 549.10^{-6}$$

Initial tensile strain (measured at reinforcement level)

$$= \epsilon_{si} = 620.10^{-6}$$

At 180 days : $\epsilon_{ct} = 2109.10^{-6}$

$$\epsilon_{st} = 810.10^{-6}$$

If initial strains *were measured at* a temperature of 2°C above *the mean*, and the 180 day strains were *measured at* 2°C below the mean, a temperature error of about 24.10^{-6} would have been incurred "both ways".

The "correct" values should be:

$$\epsilon_{ci} = 573.10^{-6}$$
$$\epsilon_{si} = 596\ 10^{-6}$$

$$\epsilon_{ct} = 2085.10^{-6}$$
$$\epsilon_{st} = 825.10^{-6}.$$

Considering creep in the extreme compression fibre:

$$\phi_{c,sh} \text{ (measured)} = (2\ 109 - 549)/549 = 2{,}84$$

$$\phi_{c,sh} \text{ (corrected)} = (2\ 085 - 573)/573 = 2{,}64$$

$$= 0{,}93\ \phi_{c,sh} \text{ (measured)}$$

i.e. A 7% error has been incurred by a 4°C temperature variation.

The hypothetical example considered above presents an extreme situation, but it is evident that temperature variation can significantly affect strain results. The effect will be greater at early days when strains are smaller. Fortunately temperature does not affect deflection in the same way. It is immediately evident from the example that total differential strain ($|\epsilon_c| + |\epsilon_s|$) and curvature remain constant.

In all previous research examined the importance of control beams to monitor shrinkage deflection has been underrated. For each beam subjected to sustained loading, shrinkage deflection and strain should be monitored on a similar pre-cracked, unloaded specimen. If both beams are stored in the same environment, this will also allow the elimination of the effect of temperature variation on strain measurements. In this investigation no doubly reinforced shrinkage specimen was manufactured, so shrinkage deflections and strains had to be calculated for beam series B. The arrangement for the measurement of shrinkage deflections on beam Mk AW proved inadequate, with the result that shrinkage deflection had to be calculated from measured midspan strains for beam series A. As has been noted, this procedure is not entirely satisfactory and could have introduced inaccuracies. Further inaccuracy may have been introduced by the correction required for delayed creep recovery in beam Mk AW during the first three days of measurement.

Experimental error is difficult to eliminate in sustained loading tests. This is die to the long duration of the test and the large storage space required. Both these factors make rigid control and close supervision difficult. Once loads have been applied, any stoppages or corrections applied adversely affect the results. Some researchers (Washa and Fluck[12], Mohamedbhai and Taylor[25]) have reported experimental difficulties, but even where no problems are reported, inconsistencies in the results suggest that the experimental work was not always entirely trouble-free.

The results of this investigation may have been adversely affected by several factors:

(1) Difficulties were experienced with the calibration of the load cells. During the first few days of testing, the beams had to be repeatedly loaded and unloaded to check the calibration. This could have affected early age creep.

(2) Loads had to be adjusted periodically to counter pressure losses in the hydraulic systems and the increasing deflection due to creep.

(3) The storage environment was inadequately controlled (Refer to previous discussion on temperature effects). Humidity was not controlled at all in the beam store.

(4) As noted, the monitoring of shrinkage deflections and strains was deficient in several respects.

Despite these factors which could have adversely affected the accuracy of results, measured and calculated deflections compare very favourably. For ease of reference, the comparisons of Chapters 5 and 6 are summarised in Table 7.1. The extreme ranges of the ratio calculated deflection/measured deflection for each calculation method and each set of results are presented. Only the 180 day results of this investigation are given.

Table 7.1 Range of calculated/measured long term deflection for different calculation methods and research results

Long term deflection excluding shrinkage			
Calculation Method	CP110	Neville	Proposed
Washa and Fluck: A	0,93-1,00	1,04-1,06	1,12-1,21
B	0,79-0,81	0,78-0,80	0,98-1,02
Corley & Sozen	0,90-1,02	0,88-1,13	1,00-1,12
Bakoss et al	0,94	0,87	1,05
Current Study : A	0,84-0,87	0,85-0,88	0,94-0,97
B	0,72	0,72-0,73	0,86-0,87

Long term deflection including shrinkage	
Calculation Method	SAICE (Pretorius)
Washa and Fluck: A	1,21 - 1,31
B	1,10 - 1,16
Corley and Sozen	1,04 - 1,23
Bakoss et al	0,97
Current Study: A	0,93 - 0,96
B	0,86

8. CONCLUSION

The scope of the experimental part of this investigation has basically been limited to the examination of midspan strain and deflection development with time on two singly and two doubly reinforced rectangular concrete beams subjected to sustained loading. All other tests were performed primarily for "control" purposes. The tensile reinforcement percentage, beam dimensions, span and level of applied loading were essentially the same for all four beams. This scope is far too limited to provide absolute confirmation of the validity of the proposed calculation method.

The calculation method of Chapter 3 has been derived from a theoretical consideration of midspan strain development with time. The derivation relies partly on quantitative analysis and partly on qualitative assessment. A qualitative assessment cannot be confirmed by limited experimental observation. However, if even limited observed results compare favourably with the results of a quantitative theoretical analysis, it is likely that the theory will apply over a range limited only by the boundaries of its derivation.

Thus, because of the limited scope of the experimental part of this investigation and the limited benefit derived from the examination of the results of other researchers, conclusions drawn regarding hypotheses based on qualitative assessment need to be confirmed by a far more comprehensive study, and should be viewed with caution. However, conclusions drawn regarding hypotheses based on quantitative analysis are likely to have universal application (see section 8.3).

8.1 PREDICTION OF CONCRETE PROPERTIES

Very limited coverage has been given to the prediction of concrete elastic modulus and creep and shrinkage characteristics in this investigation. The concrete mix used exhibits high shrinkage and a low elastic modulus. The wide deviation of the measured values from the values predicted or recommended by current codes of practice and popular calculation methods emphasizes the necessity of measuring these parameters where deflections are critical. Long term shrinkage and creep characteristics can probably be more accurately predicted by extrapolation from short term measurements than by calculation from mix constituents and environmental conditions.

8.2 SHRINKAGE DEFLECTIONS

In this study the emphasis has been on long term deflections due to creep. Shrinkage strains have been measured to calculate shrinkage deflection so that this variable may be deducted from the total measured deflection. Very little attention has been given to the prediction of shrinkage deflection from free shrinkage strain measured on control prisms. The recommendations of CP110 compare favourably with measured shrinkage deflections in this study and also in the tests performed by Bakoss, but underestimate shrinkage deflection as measured by Corley and Sozen. The equivalent tensile force method recommended by Hobbs significantly overpredicts shrinkage deflection in all the cases studied. It should be borne in mind, though, that the concrete used in this investigation exhibits a high free shrinkage which may give a bias to the comparative calculations performed.

8.1 PREDICTION OF CONCRETE PROPERTIES

Very limited coverage has been given to the prediction of concrete elastic modulus and creep and shrinkage characteristics in this investigation. The concrete mix used exhibits high shrinkage and a low elastic modulus. The wide deviation of the measured values from the values predicted or recommended by current codes of practice and popular calculation methods emphasizes the necessity of measuring these parameters where deflections are critical. Long term shrinkage and creep characteristics can probably be more accurately predicted by extrapolation from short term measurements than by calculation from mix constituents and environmental conditions.

8.2 SHRINKAGE DEFLECTIONS

In this study the emphasis has been on long term deflections due to creep. Shrinkage strains have been measured to calculate shrinkage deflection so that this variable may be deducted from the total measured deflection. Very little attention has been given to the prediction of shrinkage deflection from free shrinkage strain measured on control prisms. The recommendations of CP110 compare favourably with measured shrinkage deflections in this study and also in the tests performed by Bakoss, but underestimate shrinkage deflection as measured by Corley and Sozen. The equivalent tensile force method recommended by Hobbs significantly overpredicts shrinkage deflection in all the cases studied. It should be borne in mind, though, that the concrete used in this investigation exhibits a high free shrinkage which may give a bias to the comparative calculations performed.

8.3 MIDSPAN STRAINS

The proposed calculation method is based on theoretical midspan strain development with time. In Chapter 3 several significant hypotheses were put forward in the derivation of this method. Measured and predicted strains were compared in Chapter 5. Each hypothesis is examined independently below with regard to experimental correlation and theoretical validity. For the reasons given in Chapter 6, the midspan strain measurements of the other researchers[(7), (12), (13)] are of very little use in this regard.

(1) Calculations are based on the fully cracked beam section.

This is an approximation. The fully cracked condition is not necessarily achieved immediately after loading. Observations indicate that beams substantially cracked under initial loading approach this condition after a short time (as related to time in long term deflection calculations) under sustained load. The beams of this investigation became effectively fully cracked within one month of load application, and those of Corley and Sozen[(13)] took only ten days to reach this condition.

This hypothesis has not been substantiated by calculation and needs to be confirmed by a far more comprehensive study. The application of the proposed calculation method should be limited to beams substantially cracked under initial loading.

(2) Plane sections remain plane after loading.

This hypothesis is confirmed by all the research results studied in this investigation and supports the use of elastic theory in initial deflection calculation.

(3) Deflections calculated from midspan strains.

The proposed calculation method is derived from a theoretical evaluation of the development of midspan strains with time. Inherent in this derivation is the assumption that deflections can be calculated from midspan strains. Unfortunately this has not been verified experimentally. Deflections calculated from measured strains exhibit considerable scatter when compared with measured deflections. This presumably results from the erratic crack pattern produced in the beam tension zone. This does not necessarily invalidate the proposed calculation method, but it does mean that a good correlation cannot be expected between calculated and measured strains.

(4) Strain development in extreme compression fibre.

Measured initial compression strains closely approximate the values calculated assuming a fully cracked beam section for the beams of this study. This is expected because all beams were substantially cracked under initial loading and tension stiffening primarily affects strains in the tension zone. Initial measured compression strains were marginally less than the values calculated assuming a fully cracked section in the research of Bakoss et al[7] and Corley and Sozen[13]. This is not deemed particularly significant because these strains will rapidly increase to the cracked section values with the rapid development of cracking in the tension zone.

results studied in this investigation and supports the use of elastic theory in initial deflection calculation.

(3) Deflections calculated from midspan strains.

The proposed calculation method is derived *from* a theoretical evaluation of the *development of midspan* strains with time. Inherent *in this derivation* is the assumption that *deflections* can be calculated from midspan strains. Unfortunately this has not been *verified* experimentally. Deflections calculated from *measured* strains exhibit considerable scatter when compared with measured deflections. This presumably results from the erratic crack pattern produced in the beam tension zone. This does not necessarily invalidate the proposed calculation method, but it does mean that a good correlation cannot be expected between calculated and measured strains.

(4) Strain development in extreme *compression* fibre.

Measured initial *compression* strains closely approximate the *values* calculated assuming a fully cracked beam *section for* the beams of this study. This is expected because all beams were substantially cracked under initial loading and tension stiffening primarily affects strains in the tension zone. Initial measured compression strains were marginally less than the values calculated assuming a fully cracked section in the research of Bakoss et al[7] and Corley and Sozen[13]. This is not deemed particularly significant because these strains will rapidly increase to the cracked section values with the *rapid development of* cracking in the tension zone.

The most important innovation in the proposed calculation method is the theoretically derived development of creep strain in the extreme compression fibre with time. The theoretically predicted extreme fibre creep coefficient from Figure 3.2 compares very favourably with the measured coefficient in the singly reinforced beams of this study (refer Table 5.6). The theory was derived from a quantitative assessment and therefore should not be limited to any particular range of beam dimensions, spans or reinforcement percentages. Further investigation is required, however, to substantiate the empirical correction applied for beams with compression reinforcement.

The theory derived for compression strain development is strictly applicable only to completely cracked beam sections. The reduced creep coefficient (as compared with the prism creep coefficient) is derived from the variation of neutral axis depth with creep. The theory could be adapted for substantially uncracked sections if a method is derived for the calculation of neutral axis depth in such sections.

(5) Strain development at level of tension reinforcement.

The proposed calculation method is based on the fully cracked beam section and zero tensile strain increase with time at the level of the tension reinforcement. Both asssumptions or hypotheses are approximations, but are in good agreement with the measurements made in this investigation. Again, a more comprehensive investigation is required for beams substantially uncracked under initial loading.

8.4 DEFLECTIONS

The comparisons between measured and calculated deflections of Chapters 5 and 6 are summarised in Table 7.1. Care has been taken to apply the calculation methods as intended by the authors. All the methods examined give reasonable results. The ratio of calculated/measured deflection for individual results ranges between 0,72 (CP110 - Current Study B) to 1,31 (SAICE - Washa and Fluck A).

For long term deflection excluding shrinkage the methods of CP110 and Neville give very similar results although both marginally underestimate. The calculation method proposed in Chapter 3 generally gives better results than these methods. It is interesting to note that the degree of underestimation by the much maligned CP110 method is small. The method recommended by the Deflection Committee of the SAICE gives good results in the calculation of long term deflections including shrinkage.

For the research results examined in this study, making use of shrinkage and creep characteristics measured on control prisms and adjusting these properties for the different storage conditions and volume/surface ratios of the companion beams (by the recommendations of ACI 209), the calculation method proposed in Chapter 3 gives better results than the other calculation methods examined.

9. RECOMMENDATIONS

9.1 CALCULATION METHOD

It must be emphasized that the calculation method developed in Chapter 3 should only be applied to beams substantially cracked under initial loading. As noted previously, this limitation is not as severe as it appears because deflections are not likely to be a problem in uncracked members, and deflection checks are generally only required in highly reinforced, heavily loaded, long span elements.

The proposed calculation method has essentially bee developed to improve accuracy in long term deflection calculations where concrete properties (creep, shrinkage, elastic modulus) have either been measured on control prisms or have baen calculated by a proven method for the mix design used. If mix proper- ties are estimated, it is doubtful whether this calcu- lation method has any significant benefit over the other calculation methods examined here. In such instances it is probably easiest to use the method proposed by the SAICE with a creep coefficient read from the C & CA 3 curves. This method is easier to apply since it avoids the calculation of the shrinkage properties of the mix. Generally tha CP110 and Neville methods should be avoided because they tend to underestimate long term deflection, and in most cases an upper bound deflection value will be sought. The CP110 method also requires performing the cracked section modular ratio calculations twice, first to calculate initial deflection and then to calculate long term deflection using the reduced elastic modulus and increased modular ratio. The equations involved are complex, making calculation errors possible.

If the deflection related properties of a concrete mix can be determined to a reasonable degree of accuracy, it is recommended that the method proposed in Chapter 3 be used to calculate long term deflection excluding shrinkage. Shrinkage deflection should be calculated by the method prescribed by CP110. For completeness, the recommended method is outlined below:

<u>Recommended Method of Long Term Deflection Calculation</u>

1. Determine the degree of cracking under maximum load in the reinforced concrete element to be considered. As a very rough guide, the element may be considered "substantially cracked" where

   $$(I_e - I_{cr})/(I_g - I_{cr}) \leq 0,5 \qquad (9.1)$$

   and I_g = second moment of area of gross concrete section

   I_{cr} = second moment of area of transformed cracked section

   I_e = effective second moment of area (equation 2.4)

   If the element is not substantially cracked under maximum loading, the calculation method recommended here is likely to overestimate total long term deflection. In such situations it is recommended that an alternative calculation method catering for tension stiffening (eg. CP110) is used.

2. Determine ϕ_{ct} and ϵ_{sht} by measurement on control prisms or by a proven calculation method for the

mix to be used. The methods recommended by ACI 209 should be adequate for extrapolating short term measurements to determine extreme long term values. Measured prism coefficients must be adjusted to account for the different storage environment and volume/surface ratio of the element under consideration. The methods of ACI 209 should be suitable for this adjustment too.

3. Calculate x_i and Δ_i for the completely cracked section.

4. Factor ϕ_{ct} by $1/(1 + 50\rho')$ to allow for compression reinforcement.

5. From x_i and ϕ_{ct} (factored) from (4) determine ϕ'_{ct} from the curves of Figure 3.2.

6. Then:

$$\Delta_t = (1 + x_i.\phi'_{ct})\ \Delta_i \qquad (9.2)$$

7. Calculate Δ_{sh} by method of CP110.

Total long term deflection = Δ_t (eqn.9.2) + Δ_{sh}

9.2 FURTHER RESEARCH

It has been noted previously that the scope of the experimental part of this research has been too limited to provide absolute confirmation for the hypotheses of Chapter 3. The theory proposed needs to be confirmed by a more detailed research programme. Apart from this general deficiency, other areas of research can be identified to complement this investigation and possibly provide a universally applicable deflection theory.

The additional research prescribed here does not necessarily require an experimental investigation. Considerable research information exists for long term deflections, and it may be possible to solve some of the problems outlined below by a study of existing literature.

Total long term deflection can be divided into four components, initial deflection, deflection due to creep, deflection due to shrinkage and an additional component due to the increase of cracking in the tension zone. Initial deflection can be accurately predicted using the partially cracked section concept. For sections substantially cracked under initial loading the additional component due to increased cracking is merely the difference between the initial deflection and the deflection calculated assuming a fully cracked section. Creep deflection can be calculated by the theory proposed in Chapter 3.

Further research is required for beams substantially uncracked under initial loading. In such beams the additional component due to cracking may be reduced, and it may be necessary to derive creep deflection from the partially cracked section.

Further research into shrinkage deflection is also required. It has been noted previously that every beam subjected to sustained loading in tests should be accompanied by a similar unloaded "control" member to monitor shrinkage. It is possible that a method of calculating shrinkage deflection from strain adjustment can be derived.

The effect of compression reinforcement on creep in the compression zone requires further investigation. The recommendation of Branson[8] has been used in the proposed calculation method to allow for this effect, but the choice of method has not been substantiated. Pretorius[6] uses a different method in his calculations.

REFERENCES

(1) CP110 - 1972. Code of Practice for the Structural Use of Concrete, British Standards Institution, November 1972.

(2) ACI 318 - 1983. Building Code Requirements for Reinforced Concrete, ACI, Detroit, 1983.

(3) SABS 0100 - 1980. Code of Practice for the Structural Use of Concrete, SABS, Pretoria, 1980.

(4) Bate, S.C.C. et al. Handbook on the Unified Code for Structural Concrete (CP110- 1972), Cement and Concrete Association, 1972.

(5) Neville, A.M., Dilger, W.H., Brooks, J.T. Creep of Plain and Structural Concrete, first edition, New York, Longman Inc., 1983.

(6) Pretorius, P.C. Proposed calculation method for deflections, The Civil Engineer in South Africa, Vol 27, No 6, June 1985.

(7) Bakoss S.L. et al. Long term deflections of reinforced concrete beams, Magazine of Concrete Research, Vol 34, No 221, December 1982.

(8) Branson, D.E. Compression Steel effect on long-time deflections, ACI Journal, Proceedings Vol 68, No 8, August 1971

(9) Mayer, H. Die berechnung der durchbiegung von stahlbeton - bauteilen, Deutscher Ausschuss fur Stahlbeton, No 194, 1967

(10) Trost, H. The Calculation of Deflections of Reinforced Concrete Members - a Rational Approach, ACI SP -76, Detroit, 1982.

(11) Parrott, L.J. Simplified Methods for Predicting the Deformation of Structural Concrete, Development Report 3, Cement and Concrete Association, October 1979.

(12) Washa, G.W. & Fluck, P.G. Effect of compressive reinforcement on the plastic flow of reinforced concrete beams, ACI Journal, Proceedings Vol 49, No 2, October 1952.

(13) Corley, W.G. & Sozen, M.A. Time dependant deflections of reinforced concrete beams, ACI Journal, Proceedings Vol 63, No 17, March 1966.

(14) Bayazid, H & Pauw, A. Creep and Shrinkage of Eccentrically Loaded Prisms, Report 68-15, Missouri Co-operative Highway Research Programme, Department of Civil Engineering, University of Missouri, 1968.

(15) SABS Method 863. Compressive Strength of Concrete, SABS, Pretoria, November 1976.

(16) Neville, A.M. Properties of Concrete, third edition, Bath, Pitman Publishing Inc., 1981.

(17) Davis, D.E. The Concrete Making Properties of South African Aggregates, PhD Thesis, University of the Witwatersrand, Johannesburg, 1975.

(18) ACI Committee 209. Designing for Creep and Shrinkage in Concrete Structures, ACI SP - 76, Detroit, 1982.

(19) Comite Europeen du Beton - Federation Internationale de la Precontrainte. Model Code for Concrete Structures, CEB - FIP, 1978.

(20) Alexander, M.G. Prediction of elastic modulus for design of concrete structures, The Civil Engineer in South Africa, Vol 27, No 6, June 1985.

(21) Alexander, M.G. Shrinkage of Concrete, University of the Witwatersrand, unpublished.

(22) Comite Europeen du Beton - Federation Internationale de la Precontrainte. International Recommendations for the Design and Construction of Concrete Structures, C and CA, London, 1970.

(23) Alexander, M.G. Creep of Concrete, University of the Witwatersrand, unpublished.

(24) Hobbs, D.W. Shrinkage Induced Curvature of Reinforced Concrete Members, Development Report 4, Cement and Concrete Association, Slough, 1979.

(25) Mohamedbhai, G.T.G. & Taylor,R. The long-term behavior of one-way spanning slabs under variable loading, Institution of Civil Engineers, Proceedings Vols 56 & 57, 1974.

APPENDIX A. MEASURED CREEP AND SHRINKAGE STRAINS IN PRISMS

Notes

1. All strain values quoted are in units of microstrain.

2. Initial strains:

   MkA: 459 MkB: 478 Ave: 469

3. (mod) implies modified according to ACI 209 Recommendations for different R.H. and specimen size for beams.

   Modification Factors : Creep = 1.1078 , Shrinkage = 1.2209

4. Applied stress *in creep* tests = 10MPa.

5. Each creep value represents the average for 6 prisms loaded *in* a single creep frame.

6. Each shrinkage value represents the average for 3 *prisms*.

7. Time is measured from the date of loading (creep) or end of curing (shrinkage).

TIME (days)		28	60	90	120	180
	ϵ_{sh}	322	488	561	555	633
	ϵ_{sh}(mod)	393	596	685	676	773
MK A	$\epsilon_{c,sh}$	850	1165	1338	1437	1599
	ϵ_c	528	678	777	882	966
	ϵ_c(mod)	585	751	861	977	1070
	ϕ_c(mod)	1.275	1.636	1.876	2.129	2.331

APPENDIX A. (CONT.)

MK B	ϵ_{sh}	309	459	504	521	604
	ϵ_{sh}(mod)	377	[illegible]	615	636	737
	$\epsilon_{c,sh}$	888	1136	1301	1376	1544
	ϵ_c	579	677	797	855	940
	ϵ_c(mod)	641	750	883	947	1041
	♦c(mod)	1.341	1.569	1.847	1.981	2.179
Averages	ϵ_{sh}	316	474	538	538	619
	ϵ_{sh}(mod)	385	578	657	657	755
	$\epsilon_{c,sh}$	869	1151	1320	1407	1572
	ϵ_c	553	678	787	869	953
	ϵ_c(mod)	613	751	872	963	1056
	♦c(mod)	1.307	1.599	1.859	2.053	2.255

APPENDIX B MEASURED STRAINS AT BEAM MIDSPAN

Notes

1. Depth in mm is measured from the extreme compression fibre.

2. Figures at 0 and 150 are extrapolated considering an "ideal" beam depth of 150 mm.

3. -ve implies compression and +ve tension.

4. Values for beam MK AW are corrected for delayed creep recovery. (Refer Appendix D for correction factors).

5. All values quoted are in units of microstrain.

B1 TOTAL STRAIN

Time (days)	depth	0	28	60	90	120	180
MK A1	0	-549	-1452	-1759	-1910	-2019	-2.09
	15	-412	-1180	-1456	-1592	-1684	-1768
	40	-176	-740	-956	-1072	-1136	-1200
	65	40	-268	-444	-528	-560	-616
	90	26[illegible]	200	72	-4	-1	-60
	135	684	992	968	948	992	960
	150	821	1264	1271	1266	1327	1301
MK A2	0	-573	-1482	-1777	-1928	-2030	-2119
	15	-424	-1200	-1464	-1600	-1688	-1768
	40	-196	-744	-960	-1076	-1136	-1204
	65	96	-220	-384	-472	-520	-576
	90	292	172	64	4	-16	-48
	135	764	1056	1036	1020	1048	1036
	150	913	1338	1349	1348	1390	1387

APPENDIX B1. (CONT.)

Time (days)	depth	0	28	60	90	120	180
	0	-554	-1052	-1155	-1218	-1246	-1240
	15	-400	-808	-900	-960	-976	-972
	40	-176	-440	-524	-580	-584	-576
MK B1	65	60	-20	-76	-128	-104	-104
	90	356	320	316	284	312	308
	135	828	1144	1136	1104	1180	1168
	150	982	1388	1391	1362	1450	1435
	0	-511	-1009	-1116	-1198	-1232	-1248
	15	-384	-800	-896	-972	-996	-1012
	40	-152	-428	-516	-580	-584	-604
MK B2	65	52	-52	-112	-164	-156	-172
	90	264	256	212	168	192	180
	135	628	872	860	832	888	872
	150	755	1081	1080	1058	1124	1107
	0	--	-322	-511	-601	-666	-649
	15	--	-289	-462	-545	-597	-581
	40	--	-202	-355	-427	-454	-441
MK AW	65	--	-196	-321	-389	-393	-383
	90	--	-147	-243	-303	-282	-274
	135	--	-22	-73	-100	-42	-41
	150	--	11	-24	-44	27	27

APPENDIX B2 EXTREME FIBRE STRAINS WITH SHRINKAGE DEDUCTED

Notes

1. Shrinkage strains can only be deducted for MK A beams Shrinkage strains in the MK B beams are affected by the compression reinforcement.

Time (days)		0	28	60	90	120	180
MK AW	Comp.	0	- 322	- 511	- 601	- 666	- 649
	Tens.	0	11	- [illegible]	- 44	27	27
MK A1	Comp.	-549	-1130	-1248	-1309	-1353	-1460
	Tens.	821	1253	1295	[illegible]	1300	1274
MK A2	Comp.	- 573	-1160	-1266	-1327	-1364	-1470
	Tens.	913	1327	1373	1392	1363	1360

APPENDIX C.MEASURED DEFLECTIONS

Notes

1. All values quoted are in mm.

2. The derivation of shrinkage deflections is explained in Appendix D.

BEAM MK A1						
Time(days)	0	28	60	90	120	180
Total	4.89	9.58	10.56	11.07	11.62	11.83
Initial	4.89	4.89	4.89	4.89	4.89	4.89
Shrinkage	-	1.25	1.82	2.05	2.44	2.55
Creep	-	3.44	3.85	4.13	4.29	4.39
In.+Creep	4.89	8.33	8.74	9.02	9.18	9.28

BEAM MK A2						
Time(days)	0	28	60	90	120	180
Total	5.09	9.59	10.64	11.19	11.72	11.92
Initial	5.09	5.09	5.09	5.09	5.09	5.09
Shrinkage	-	1.25	1.82	2.05	2.44	2.55
Creep	-	3.25	3.73	4.05	4.19	4.28
In.+Creep	5.09	8.34	8.82	9.14	9.28	9.37

APPENDIX C. (CONT.)

BEAM MK B1						
Time(days)	0	28	60	90	120	180
Total	4.78	7.63	8.27	8.44	8.80	8.77
Initial	4.78	4.78	4.78	4.78	4.78	4.78
Difference	-	2.85	3.49	3.66	4.02	3.99

BEAM MK B2						
Time(days)	0	28	60	90	120	180
Total	4.30	7.50	7.91	8.11	8.54	8.55
Initial	4.30	4.30	4.30	4.30	4.30	4.30
Difference	-	3.20	3.61	3.81	4.24	4.25

APPENDIX D SHRINKAGE DEFLECTIONS

A more detailed description of the derivation of shrinkage deflection is given in Section 5.2.3.

Notes

1. Shrinkage deflections are factored to allow for initial creep.

   Time = 3 days is used as a reference.

   3 day prism shrinkage values :

   Mk A = $90*10^{-6}$, Mk B = $77*10^{-6}$, AVE. = $84*10^{-6}$ (ϵ_3)

   Modification factor = F = $\epsilon_t/(\epsilon_t-\epsilon_3)$ $\Delta_{sh}' = F*\Delta_{sh}$

2. All strain values are in units of microstrain. Deflections are measured in mm.

3. (mod) implies modified according to ACI 209 Recommendations for different R.H. and specimen size for beams.

   Modification factor = 1.2209

4. Values quoted are averages for MK A and MK B prisms.

5. Δ_{sh} is calculated from midspan strains measured on beam MK AW.

Time (days)		28	60	90	120	180
	ϵ_{sh}	316	474	53	538	619
Averages (strains)	ϵ_{sh}(mod)	385	578	657	657	755
	F	1.3621	1.2151	1.1850	1.1850	1.1570
MK AW (deflect.)	Δ_{sh}	0.92	1.48	1.73	2.06	2.20
	Δ_{sh}'	1.25	1.82	2.05	2.44	2.55